CONTACTING WEB BIAXIAL STRESS TRANSDUCER

By

MICHAEL ALLEN MAGILL

Bachelor of Science in Mechanical Engineering

Oklahoma State University

Stillwater, Oklahoma

1980

Submitted to the Faculty of the
Graduate College of the
Oklahoma State University
in partial fulfillment of
the requirements for
the Degree of
MASTER OF SCIENCE
July, 1988

CONTACTING WEB BIAXIAL

STRESS TRANSDUCER

Thesis Approved:

Thesis Adviser

Dean of the Graduate College

ACKNOWLEDGMENTS

I would like to thank Dr. Keith Good for being an individual who is very pleasant to work for. It was a pleasure to think and brainstorm with him throughout the project. I look forward to getting to know him as a colleague. My thanks also go to Dr. R.L. Lowery and Dr. G.E. Young for serving on my committee.

I can't say thanks enough to my brother, Scott, for sacrificing his brand new camcorder. Sorry for the scratches! I appreciate Ray Neathery's wisdom, Larry Simmon's concern, Arlin Harris's ideas, and the "Thursday Morning Group's" support.

Finally, to my favorite person in the whole world, my wife, Lisa, who played so many roles during this project, I want to say, "Thank you! How blessed I am!"

TABLE OF CONTENTS

Chapter ... Page

I. INTRODUCTION 1

Objectives. 2
Literature Survey 3
Measurement. 3
Analysis 8
Organization. 8

II. PROCEDURE. 9

The Transducer. 9
Vacuum Ring. 10
Displacement Rod and Circular Boundary Plate 13
Deflection Measurement 16
The Frame. 18
The Web 22
Static Testing 22
Dynamic Testing. 24
Data Collection 24
Static Testing 25
Dynamic Testing. 27

III. RESULTS. 30

Experimental. 30
Static Testing 30
Dynamic Testing. 40
Theoretical 47

IV. CONCLUSIONS. 52

Overview. 52
Recommendations 52

LITERATURE CITED. 54

APPENDIXES. 55

APPENDIX A - EFFECT OF RING OR PLATE AND GRATING NOT BEING PARALLEL. . . . 56

Chapter Page

APPENDIX B - CALCULATING OUT-OF PLANE DISPLACEMENTS IF THE LINE OF SIGHT IS NOT VERTICAL 59

APPENDIX C - DATA FROM STATIC TESTING. 61

APPENDIX D - DERIVATION OF RIVELLO'S DEFLECTION EQUATION 81

LIST OF TABLES

Table Page

I. Sample Vacuum Ring Fringe Data 32

II. Sample Vacuum Ring Deflection Data 33

III. Sample Ellipse Dimensions For A Forced Displacement 35

IV. Sample Ellipse Aspect Ratio and Tension Ratio Data 36

V. Curved Axis Roller Fringe Data and Machine Direction Tensions 44

VI. Curved Axis Roller Ellipse Data and Lateral Tensions 48

VII. Vacuum Ring Fringe Count Data (Test #1). . . . 62

VIII. Vacuum Ring Deflection Data (Test #1). 63

IX. Vacuum Ring Fringe Count Data (Test #2). . . . 64

X. Vacuum Ring Deflection Data (Test #2). 65

XI. Ellipse Dimensions For a Forced Displacement (Test #3) 66

XII. Ellipse Aspect Ratio and Tension Ratio Data (Test #3) 67

XIII. Ellipse Dimensions For a Forced Displacement (Test #4) 71

XIV. Ellipse Aspect Ratio and Tension Ratio Data (Test #4) 72

XV. Ellipse Dimensions For a Forced Displacement (Test #5) 73

XVI. Ellipse Aspect Ratio and Tension Ratio Data (Test #5) 74

Table		Page
XVII.	Vacuum Ring Fringe Count Data (Test #6). . .	75
XVIII.	Vacuum Ring Deflection Data (Test #6). . . .	76
XIX.	Vacuum Ring Fringe Count Data (Test #7). . .	77
XX.	Vacuum Ring Deflection Data (Test #7). . . .	78
XXI.	Vacuum Ring Fringe Count Data (Test #8). . .	79
XXII.	Vacuum Ring Deflection Data (Test #8). . . .	80

LIST OF FIGURES

Figure Page

1. Dancer Roll. 4

2. Various Ways to Mount Tension Rolls. 4

3. Portable Tension Transducer. 6

4. Noncontacting Tension Transducer 7

5. The Transducer 11

6. Vacuum Ring. 12

7. Vacuum Source. 14

8. Displacement Rod and Circular Boundary Plate . . 15

9. Moire' Method for Measuring Out-of-Plane Displacements. 17

10. Typical Fringe Pattern for Vacuum Ring 19

11. Typical Fringe Pattern for Forced Displacement . 19

12. The Transducer Frame 20

13. Web Crucifix Shape 23

14. Static Crucifix Machine. 26

15. Web Configuration on Dynamic Machine 28

16. Comparison of Web Deflections for Uniaxial and Biaxial Loading. 31

17. Ellipse Aspect Ratio vs. Tension Ratio (X-Direction Tension: 4-4.5 lb/in) 37

18. Ellipse Aspect Ratio vs. Tension Ratio (X-Direction Tension: 2.5-3.5 lb/in) 38

19. Ellipse Aspect Ratio vs. Tension Ratio (X-Direction Tension: 1-2 lb/in) 39

Figure		Page
20.	Effect of Web Width on Deflections	41
21.	Curved Axis Roller Tensions in Machine Direction	43
22.	Theoretical Machine Direction Stresses	45
23.	Curved Axis Roller Tensions in Lateral Direction	46
24.	Theoretical Lateral Direction Stresses	49
25.	Comparison of Theoretical Deflection Values to Actual Values	50
26.	Ring and Grating not Parallel	57
27.	Line of Sight not Vertical	60
28.	Test #3: Ellipse Aspect Ratio vs. Tension Ratio (X-Direction Tension: 1-2 lb/in)	68
29.	Test #3: Ellipse Aspect Ratio vs. Tension Ratio (X-Direction Tension: 2.5-3.5 lb/in)	69
30.	Test #3: Ellipse Aspect Ratio vs. Tension Ratio (X-Direction Tension: 4-4.5 lb/in)	70
31.	Rivello's Deflection Equation	82

CHAPTER I

INTRODUCTION

This report is a study of just one of the numerous projects currently being performed at Oklahoma State University in the area of web handling. A web is any thin, flexible material. Web handling is the process of transporting this material. Transport primarily involves the web passing over a series of different rollers while various operations are performed on the web. These operations could be anything from coating to cutting the web or from collating to spreading the web.

Controlling the web during transport is a very important part of web handling. One aspect of controlling the web is controlling the tension in the web. Before the tension can be properly controlled the tension must be known. There are various ways this can be done. Typically, the tension is measured in the direction of the web's movement. This is called the machine direction. Occasionally it becomes valuable to know the tension perpendicular to the machine direction. This is called the lateral direction. Sometimes it also becomes valuable to know the tension in a localized area on the web as opposed to an average tension across a large area .

Once the tension in a web is known it can be used to calculate the stresses. The stresses in the web are a function of the tension and the web geometry (primarily the thickness.) If the web's stresses are known, failure can be prevented. The stresses can also be used to predict strain and elongation if the modulus of elasticity is known. All of these stresses, strains, and elongations are straight forward to calculate but their accuracy is dependent on having reliable values for tension.

Objectives

The objective of this study was to develop a web tension transducer that would have the following capabilities.

1. The ability to measure tension in both the machine and lateral directions with reasonable accuracy.

2. The ability to measure tension in a localized area on the web as opposed to an average tension over a large area.

3. The tranducer must measure the tension by physically contacting the web; but, at the same time, it must not induce tension into the web.

Literature Survey

Measurement

Several devices exist that have one or two of the capabilities listed above; but, none were found that had all three capabilities. Little information was found on the topic of tension measurement in a web and the information that was available was very broad. No information was found on the specfic topic of biaxial tension measurement in a localized area.

Satas [8] discusses several tension sensing devices but all are uniaxial and give an average tension across the width of the web.

The first device Satas discusses is called a dancer roll. The dancer roll is a counter-balanced roll in contact with the web. The dancer roll can move in either direction from its null position, giving a signal to the tensioning device to either increase or decrease the tension (Figure 1).

Many different dancer roll designs are possible. The dancer roll might move vertically or horizontally, it might be pivoted and move in an arc. The advantage of dancer rolls over other tension sensing devices is that they can move and thereby dampen small disturbances in web tension.

Bak [1] discusses a dancer roll with rotary motion sensors that monitor angular position. This device is

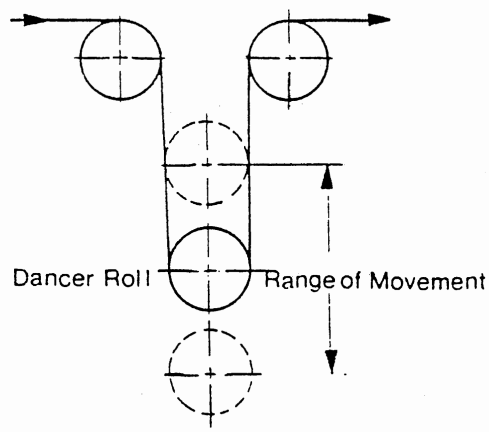

Figure 1. Dancer Roll

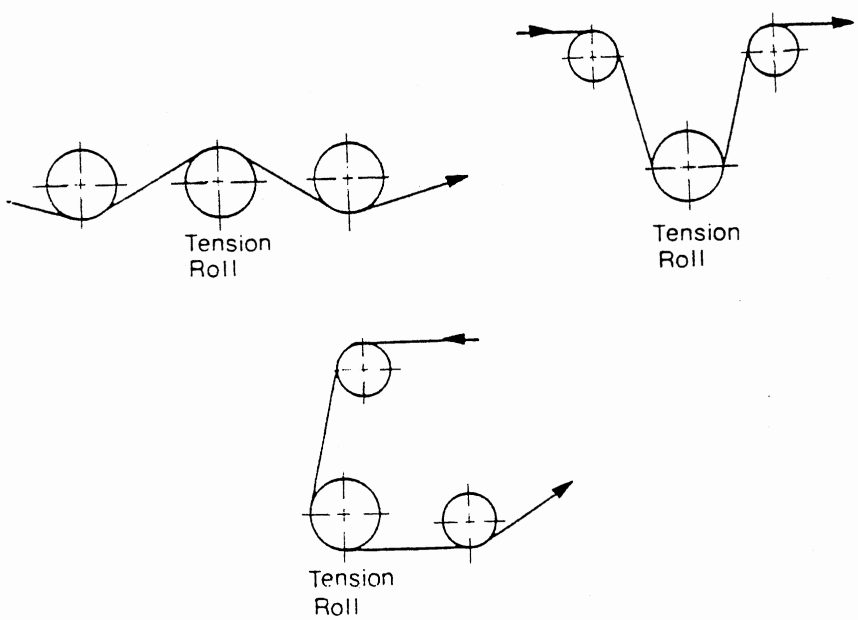

Figure 2. Various Ways to Mount Tension Rolls

also used to measure and regulate tension.

Other devices that Satas mentions are various idler rolls with load sensing devices mounted on one or both sides. These sensors can be pneumatic, hydraulic, piezoelectric, or magneto-elastic. A roll with load sensing devices on both sides is more accurate, the measured tension value does not require centering of the web and it is not affected by non-uniform web tension across the width. The tension idler rolls can be mounted in various ways as shown in Figure 2.

A portable tension transducer is discussed by Hansen [3]. The transducer (Figure 3) has a measuring head with a spring blade that presses against the web. The deflection of the spring blade is then measured with a contactless inductive displacement sensor. The output from this sensor is voltage. This voltage can then be correlated to the web tension. The transducer will measure tension in a localized area but it only measures in the direction of maximum tension.

Nutter [5] discusses a noncontact transducer (Figure 4) that is currently being developed. The transducer operates by hitting the web with a quick pulse of air and then measuring the speed of the wave it creates. The wave speed is a function of the web's density and tension. The wave travels in the direction of maximum tension so it will not work for measuring lateral tension. It appears the transducer will work

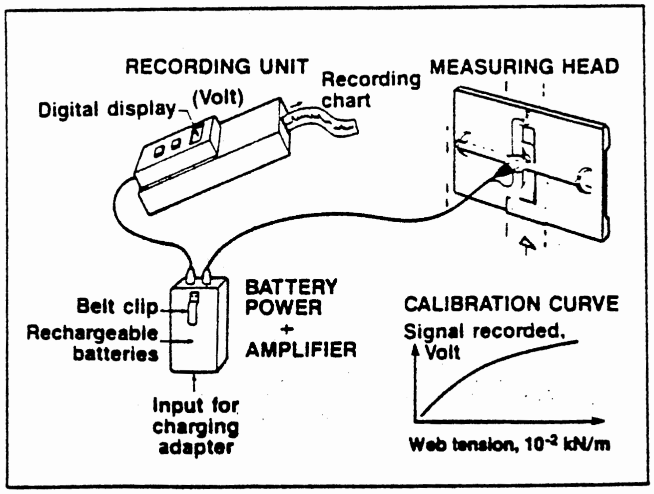

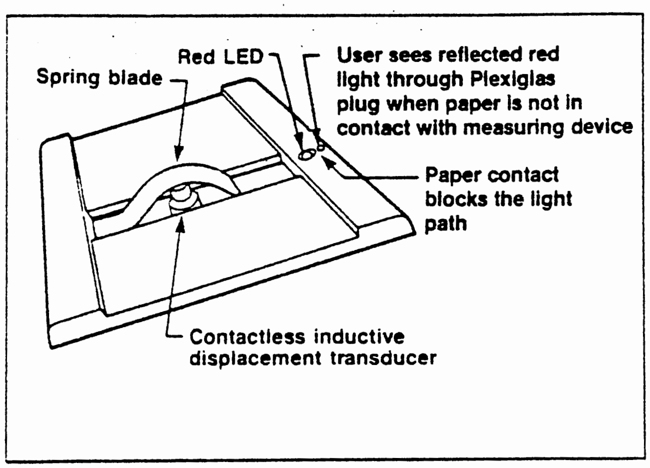

Figure 3. Portable Tension Transducer

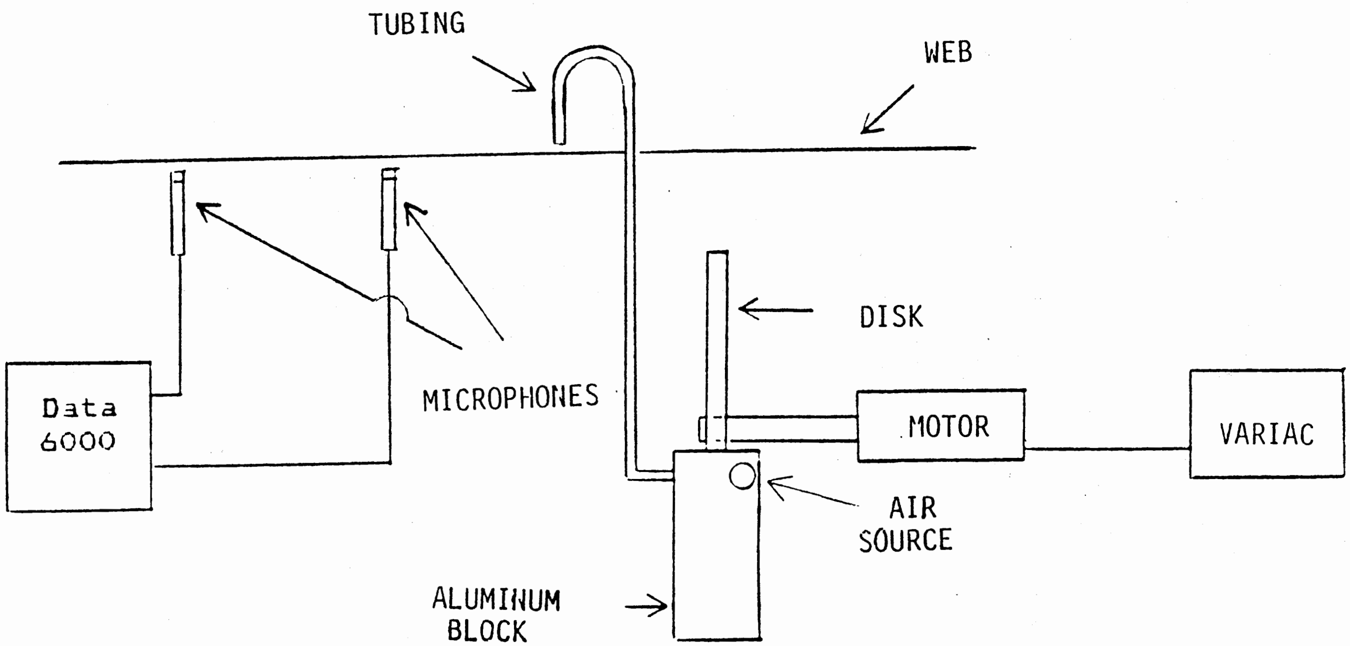

Figure 4. Noncontacting Tension Transducer

for measuring the variation in machine direction tension across the width of a web.

Analysis

The behavior of a web is characterized as a membrane. Basic membrane theory can be found in most books dealing with plate and shell structures. This study primarily used the derivations from Rivello [7]. This derivation is discussed in more detail in Chapter III and Appendix D.

Organization

The experimental procedure used in this study is in Chapter II. This procedure is broken into 3 areas, the transducer, the web, and data collection. Chapter III gives the results, both experimental and analytical. The conclusions of this study and recommendations for further study are given in Chapter IV.

CHAPTER II

PROCEDURE

The Transducer

The transducer senses the tension in the web and produces a series of light and dark optical patterns that can be correlated to tension. The transducer does this by first forcing an out of plane deflection into the web using a vacuum source. This vacuum is applied to the web through a circular ring. The amount of deflection caused by the vacuum can be used to closely approximate the maximum tension whether it is in the machine direction or lateral direction. (Henceforth, the tension will always be assumed to be greatest in the machine direction.) The lateral tension is then found by forcing a known point displacement into the web through a circular ring. This causes differing deflection slopes in the machine and lateral directions inside the circular ring. The deflections caused by the vacuum ring and point displacement are both measured using an optical method called moire' fringe. The moire' method sets up a series of optical fringe patterns which directly correspond to deflection. These deflections are then correlated to the tension in both directions. Figure 5 is a simplified sketch of how the transducer works. The major components of the transducer will now be discussed.

Vacuum Ring

The purpose of the vacuum ring is to cause a uniform pressure on the web inside a circular boundary condition. Accordingly, the ring is designed to apply a uniform and symmetrical pressure on the web. In addition, the edges on the boundary are extremely smooth so as to closely approximate roller boundary conditions and minimize friction and drag. Figure 6 is a sketch of a vacuum ring.

Three different vacuum rings are available for the purpose of determining the optimum size for different web materials. The sizes available are 1, 1-1/2, and 2 inch diameter rings. Overall, for the working tension range, 1/2 pounds per inch to 5 pounds per inch, and the various materials used, the 1 inch ring performed best. Both the 1-1/2 and 2 inch rings cause buckling at the lower tensions. The 1 inch ring also works well for measuring tension in small localized areas.

The vacuum is supplied to the ring from a controlled source. The vacuum source consists of a pump which builds vacuum in a reservoir. This reservoir supplies a precise vacuum to the ring by using a needle

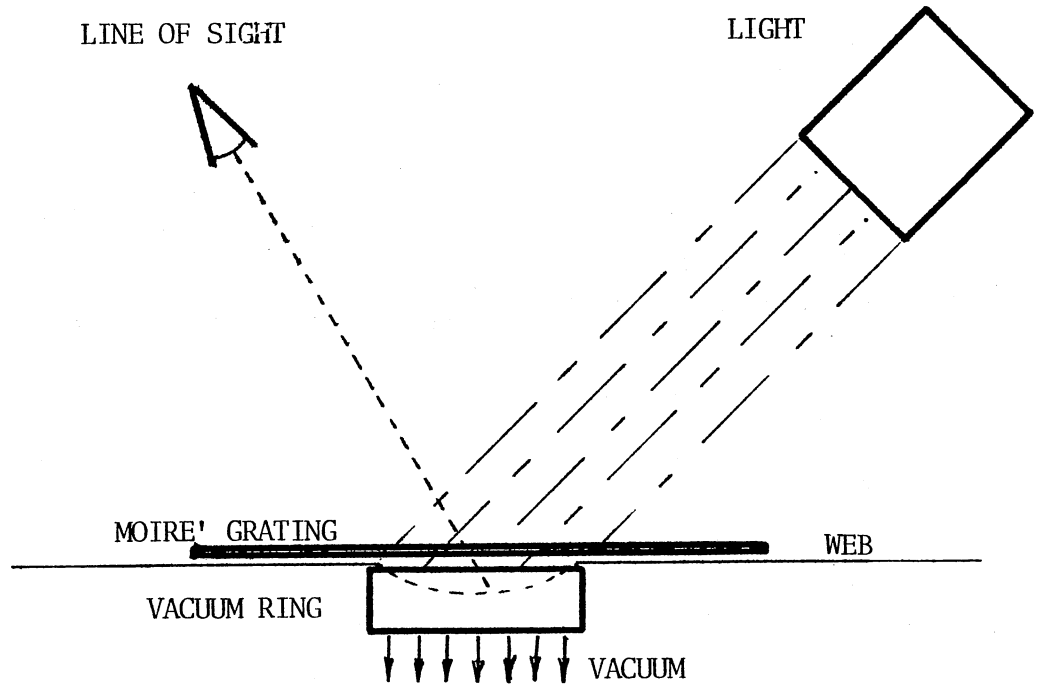

Figure 5. The Transducer

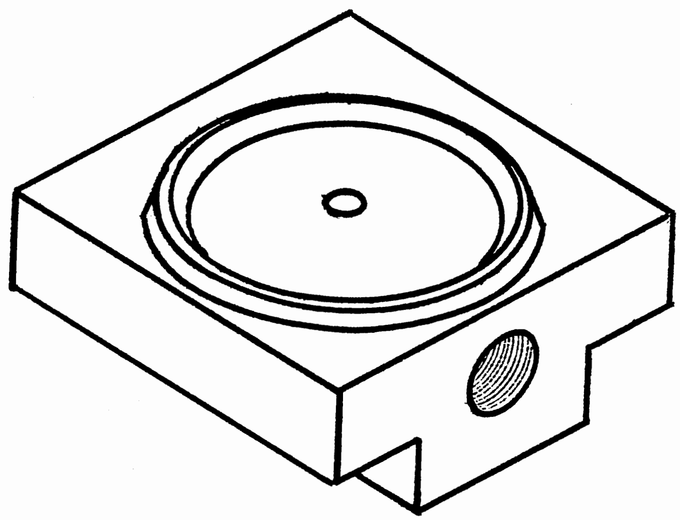

Figure 6. Vacuum Ring

valve as a regulator. The vacuum is monitored using a mercury manometer. The manometer allows the vacuum to be accurately read in the range in which the transducer is used. The manometer is located close to the ring so as to provide the best measurement of the vacuum where the web and ring contact. The leakage between the web and ring is minimal so another needle valve near the regulator valve is used as a bleed to maintain flow in the system. Figure 7 is a schematic of the vacuum source.

Displacement Rod and Circular Boundary Plate

The purpose of the displacement rod and circular boundary plate is to force a known displacement into the web through a circular hole. The rod is made from a standard micrometer caliper which is accurate to .001 inch. The spindle is ground to a hemispherical shape and polished. This provides the most uniform displacement, without inducing drag or friction. The circular boundary plate is made from a thin plate with a circular hole. The hole acts as a circular boundary. The forced displacement is placed in the center of the hole. Three different sizes of holes are available, 1/2, 3/4, and 1 inch. The 1 inch hole provides the best resolution without buckling. Figure 8 shows the displacement rod and a circular boundary plate.

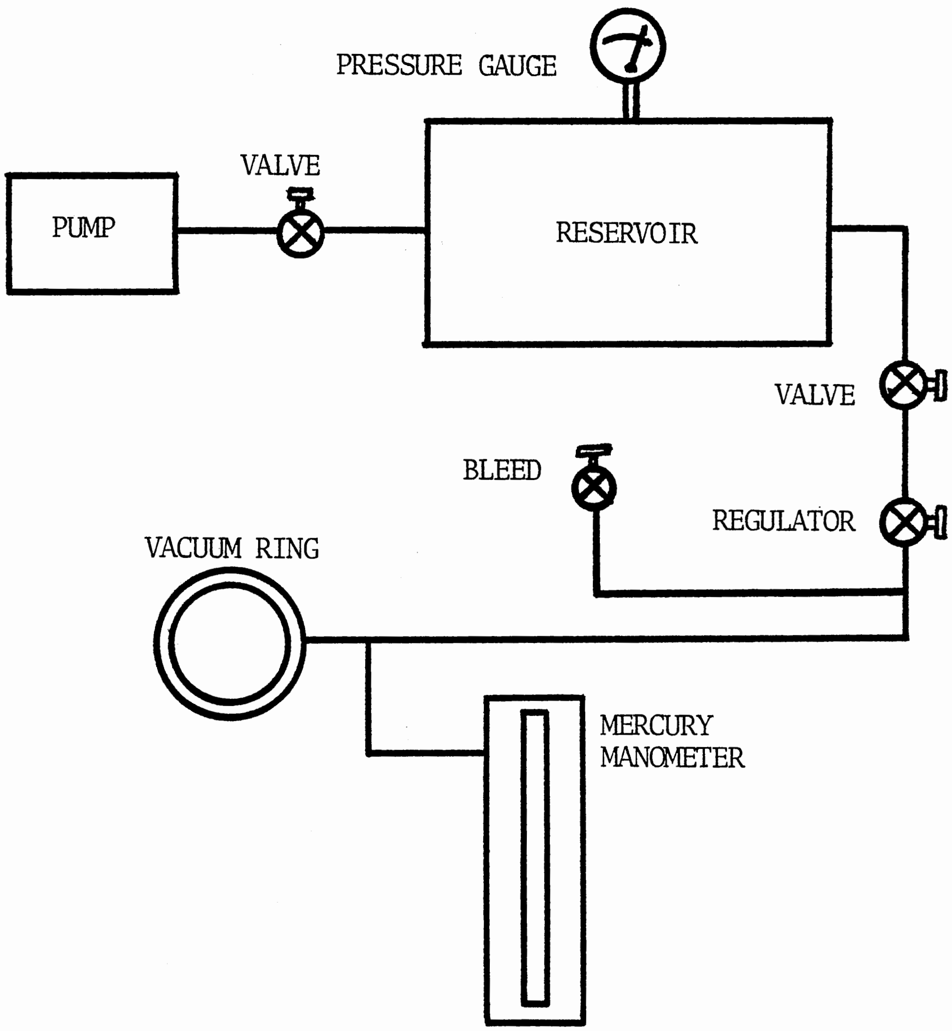

Figure 7. Vacuum Source

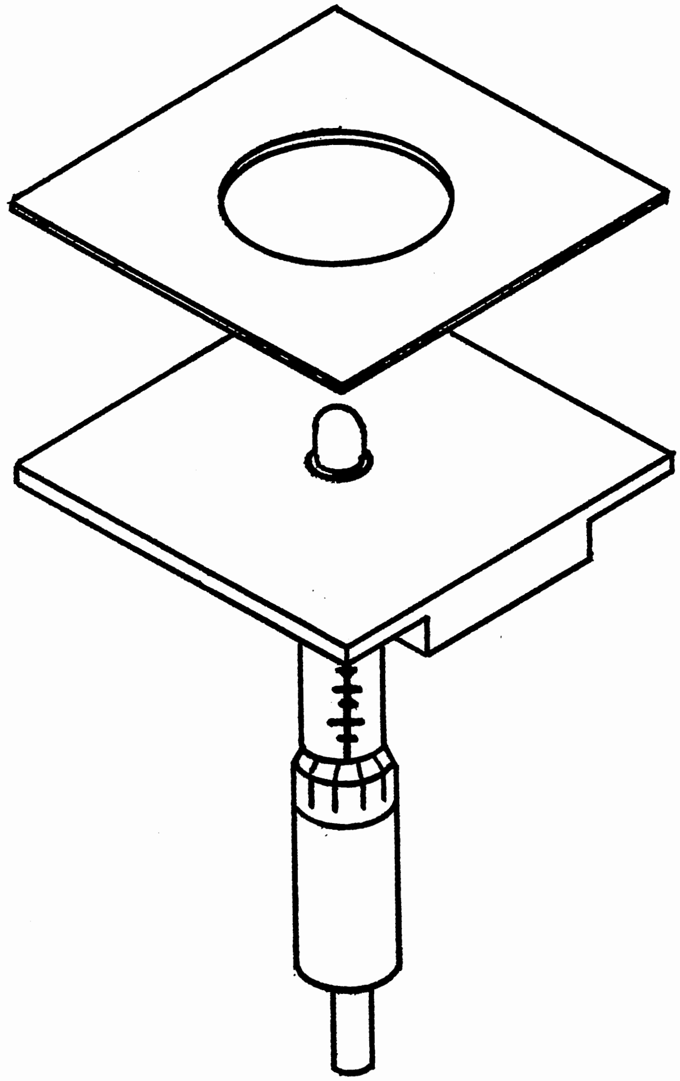

Figure 8. Displacement Rod and Circular Boundary Plate

Deflection Measurement

The deflection measurement is performed using an optical effect called moire' fringe. The method operates by shining a collimated light source through a moire' grating onto the deflected surface. The moire' grating is a sheet of glass with very small, parallel lines on the surface. The grating used in this project had 200 lines per inch. As the collimated light passes through the grating and onto the deflected surface it will cast shadows for each grating line. As the observer views the deflected surface through the grating a series of fringe patterns or dark bands will be seen if the grating and deflected surface are not parallel. Each dark band represents a relative displacement from a reference datum. Figure 9 shows the basics of how the moire' method for out-of-plane displacements works. The following equation from Dally [2] calculates the out-of-plane deplacement with reference to some datum.

$$w = np/\tan\gamma$$

where

w = out-of-plane displacement ($d_2 - d_1$)

n = order of moire' fringe at the point

p = pitch of the master grating

γ = angle of incidence of the collimated light

The light source is an overhead projector bulb with

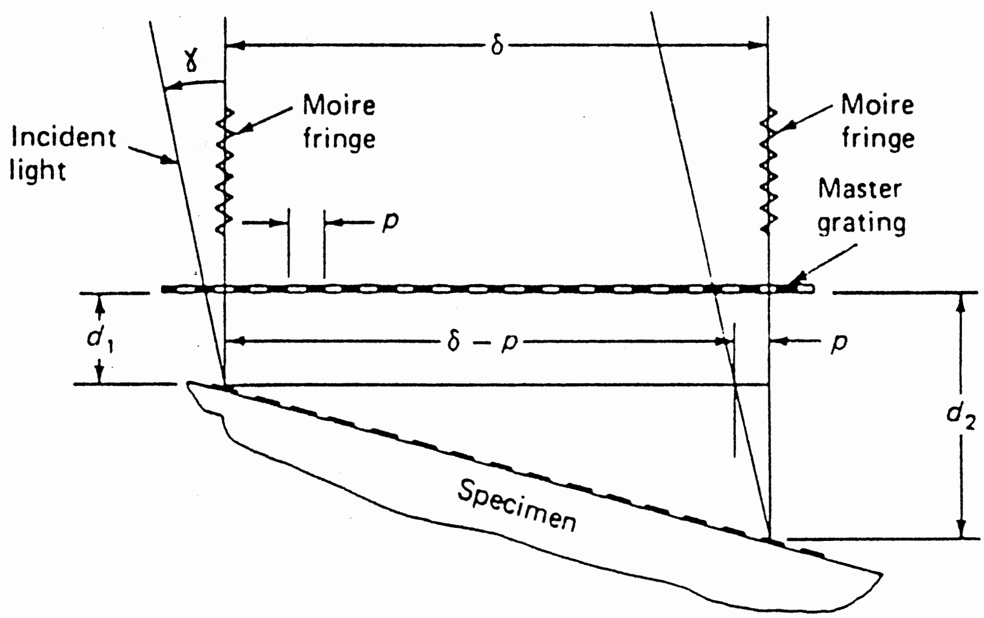

Figure 9. Moire' Method for Measuring Out-of-Plane Displacements

an aperture followed by a collimating lens. A variable voltage power source is used for varying the light intensity.

An Hitachi Camcorder is used to observe and record the fringe patterns. The light contrast on the fringe patterns is difficult to film. The Hitachi Camcorder works particularly well because it has a manual iris for adjusting to different light intensities. The filming works best if the room has no lighting except for the collimated light source. Figures 10 and 11 show typical fringe patterns from the vacuum ring and forced displacement respectively.

The Frame

The transducer frame (Figure 12) is designed to have numerous capabilities. The following is a list of capabilities of the frame.

1. The frame holds the light source, moire' master grating, and circular boundary above the web and the vacuum ring and the displacement rod below the web.

2. The frame allows for tension measurement in webs a maximum of 38 inches wide.

3. The frame holds the grating parallel to the vacuum ring and circular boundary plate to provide the best deflection measurements. The frame can be adjusted so as to insure parallelism in both directions.

4. The frame holds the light source so that the

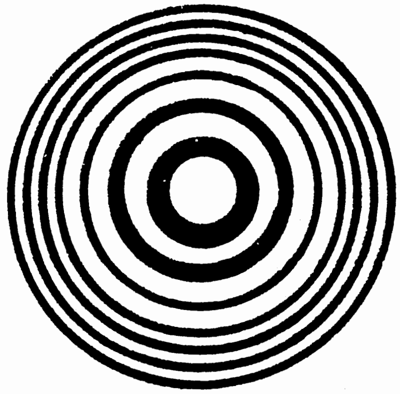

Figure 10. Typical Fringe Pattern for Vacuum Ring

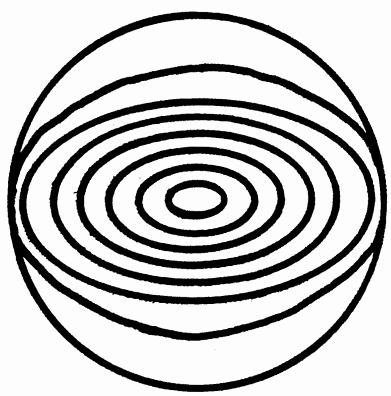

Figure 11. Typical Fringe Pattern for Forced Displacement

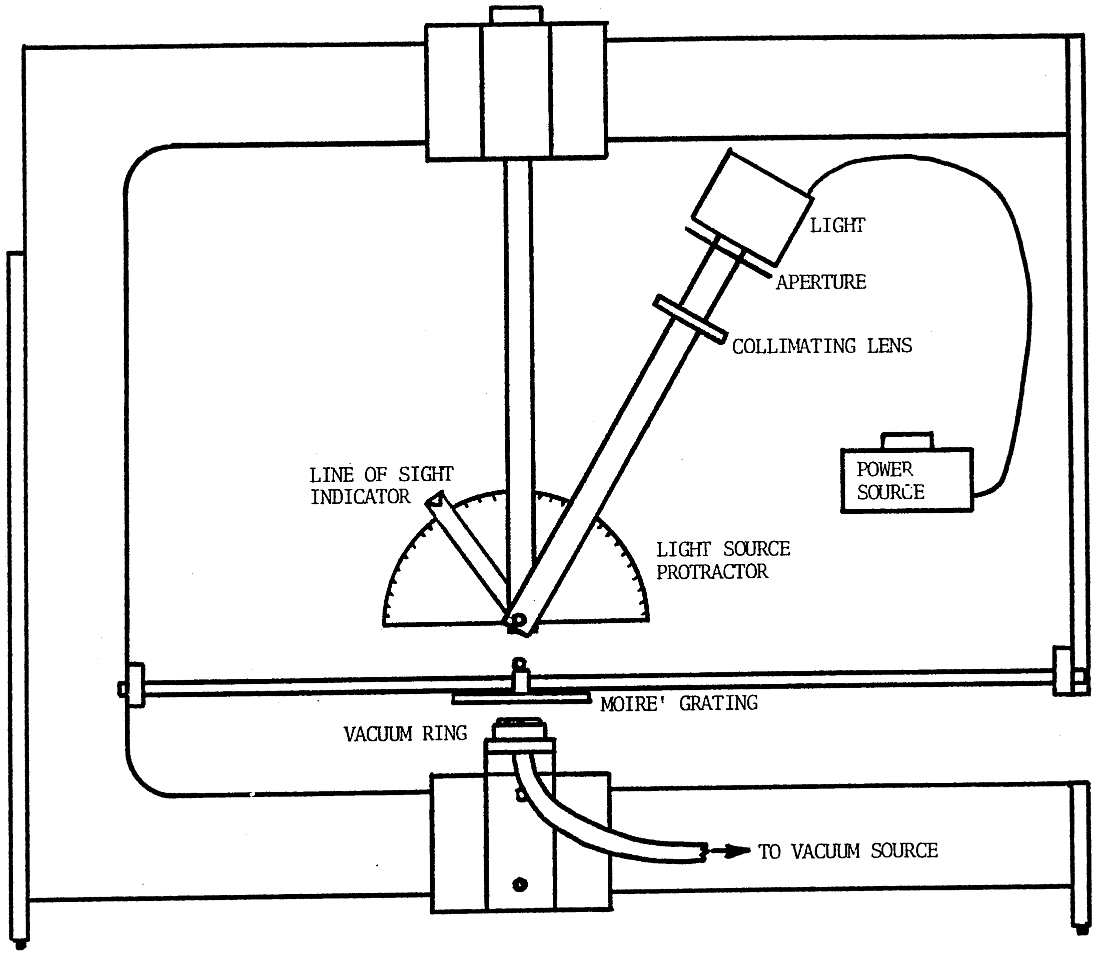

Figure 12. The Transducer Frame

aperture and collimating lens can be moved with respect to the projector bulb for focusing purposes.

5. The light source can be held and measured at any angle from the vertical.

6. The line of sight can be measured using the light source protractor.

7. The light source and grating can be slid across the length of the frame to measure the tension at any location on the web.

8. The grating can be moved from side to side and rotated in order to position the grating lines in any direction or location with respect to the light.

9. The light source can be rotated 360 degrees to position the light in any direction with respect to the grating.

10. The vacuum ring and displacement rod can be raised and lowered, slid side to side, and moved across the length of frame for positioning anywhere under the web.

11. The frame has adjustable feet to allow for leveling and to accommodate uneven surfaces.

12. The frame is made primarily out of aluminum for ease of machining and transporting.

13. The frame is rigid enough to prevent deflection and minimize vibration.

14. The camcorder is held on a separate tripod to allow flexibility of recording locations.

The Web

Static Testing

Various web geometries and material were used during the static tests. The following combinations were used.

1. Clear polyester 9 inches wide.
2. Clear polyester 18 inches wide, crucifix shape.
3. Clear polyester 6 inches wide, painted white.
4. Clear polyester 4 inches wide, painted white.
5. Clear polyester 4 inches wide, painted white, crucifix shape.
6. Polypropylene, with white acrylic coating, 6 inches wide.
7. Polypropylene, with white acrylic coating, 4 inches wide.
8. Polypropylene, with white acrylic coating, 4 inches wide, crucifix shape.

The clear polyester was approximately 0.0014 inches thick and the polypropylene was approximately 0.0016 inches thick. The contrast of the moire' fringe patterns can be greatly increased by painting the web surface white. Figure 13 shows how the crucifix web shape was cut. The shape and construction of the crucifix was critical to prevent tearing yet still give a shape that behaved as a true crucifix.

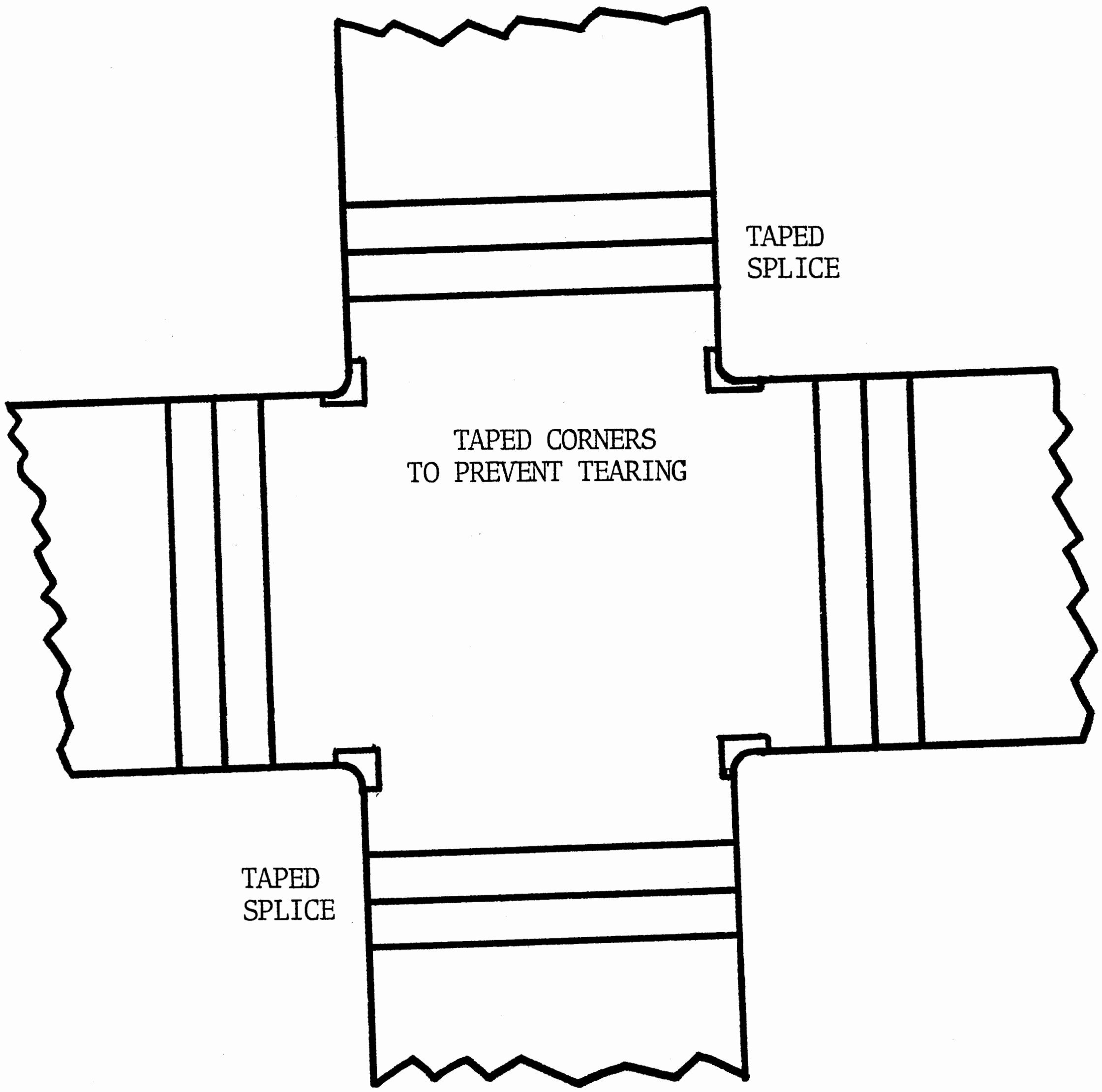

Figure 13. Web Crucifix Shape

Dynamic Testing

Two different webs were used during the dynamic testing. They were as follows:

1. Clear polyester 9 inches wide (used in preliminary friction testing).

2. Clear polyester, 26 inches wide, painted white in the location where the tension was measured.

The clear polyester was 0.0014 inches thick.

Data Collection

Several factors had to be considered to insure accurate data collection. One concern was how the deflection measurements would be affected if the vacuum ring or circular boundary plate were not parallel to the moire' grating. It was determined that if the angle between the ring or plate and the grating is small it will have no measureable effect on the deflections. The calculations used to verify this are in Appendix A.

Another factor that was considered was improving the resolution of the measurements. The resolution can be improved by increasing the number of fringes per unit displacement. The number of fringes can be increased by increasing the angle of the light source from the vertical. The number of fringes can also be increased by increasing the angle of the line of sight from the vertical. Moving the line of sight away from the vertical changes the equation for the out-of-plane displacement to the following.

$$w = np(\cos\gamma \cos\beta)/\sin(\gamma+\beta)$$

where

w = out-of-plane displacement

n = order of the moire' fringe

p = pitch of the master grating

γ = angle of incidence of the collimated light

β = angle of incidence of the line of sight

The derivation of this equation is in Appendix B.

Static Testing

Most of the testing was performed under static conditions. A static crucifix machine was used to collect the static data. Figure 14 shows a sketch of the static crucifix machine. The machine has rollers in both the machine and lateral directions. This makes it convenient for imposing tensions in both directions and calibrating the transducer.

Data was taken for various loading conditions on both the vacuum ring and the forced displacement. The data was taken in several different loading conditions for the following reasons.

1. To establish the controlling factors for the deflections.

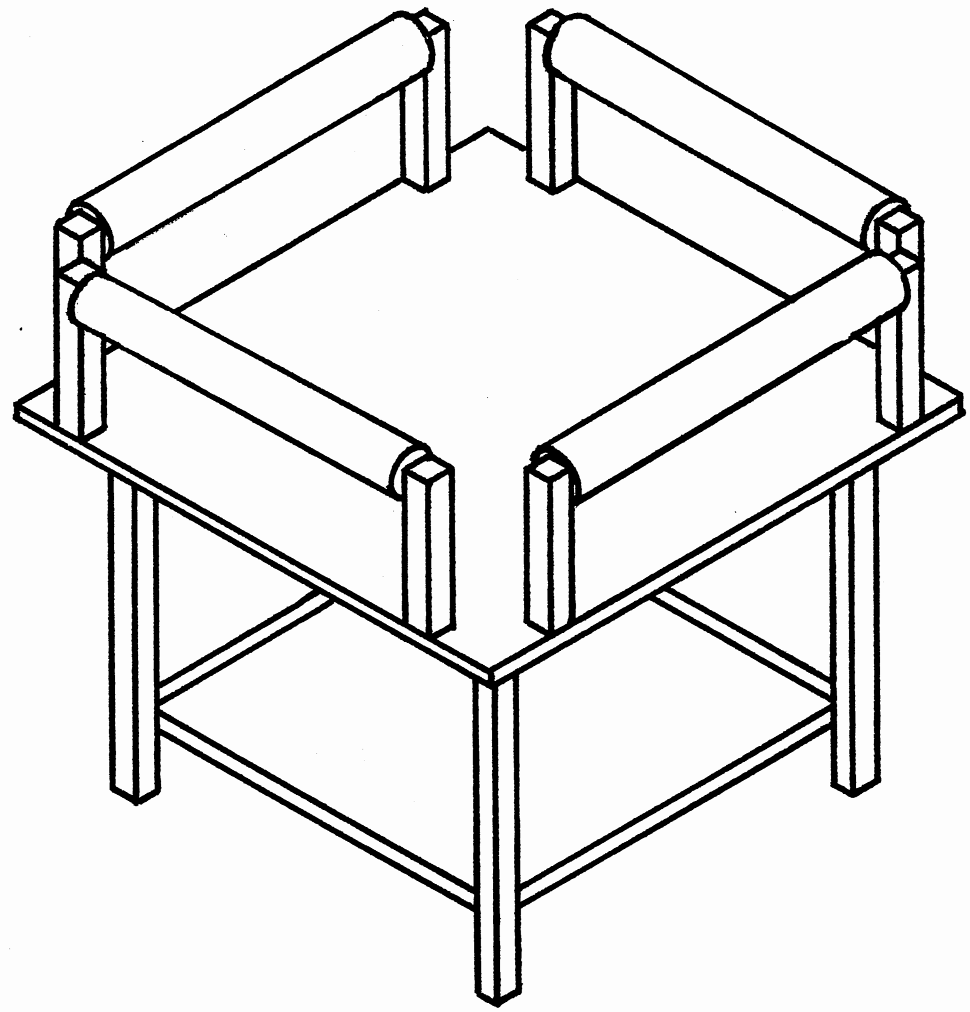

Figure 14. Static Crucifix Machine

2. To verify that the deflections can be correlated to tension in both directions.

3. To calibrate the transducer for different webs.

Dynamic Testing

Dynamic testing was conducted for the following reasons.

1. To observe the effects of friction and drag.

2. To observe the variations in tension across the width of a web on a curved axis roller.

A continuous loop web handling machine was used to perform the dynamic testing. Figure 15 is a sketch of the web configuration on the machine. The tensions were measured on the web machine in both the dynamic and static conditions. The tensions were the same in both conditions. All additional testing was performed by running the machine for a short time and then stopping it to take measurements. This allowed the web to get centered and squared on the curved axis roller but made measurement easier since the web was not moving.

The tension was measured with the curved axis roller set in two different positions. The first position was with the bow plane parallel to the incoming web. The second position was with the bow plane tilted down 45 degrees from the incoming web. The tension was measured on the incoming web 7.5 inches out from the center line of the curved axis roller. The web wrapped

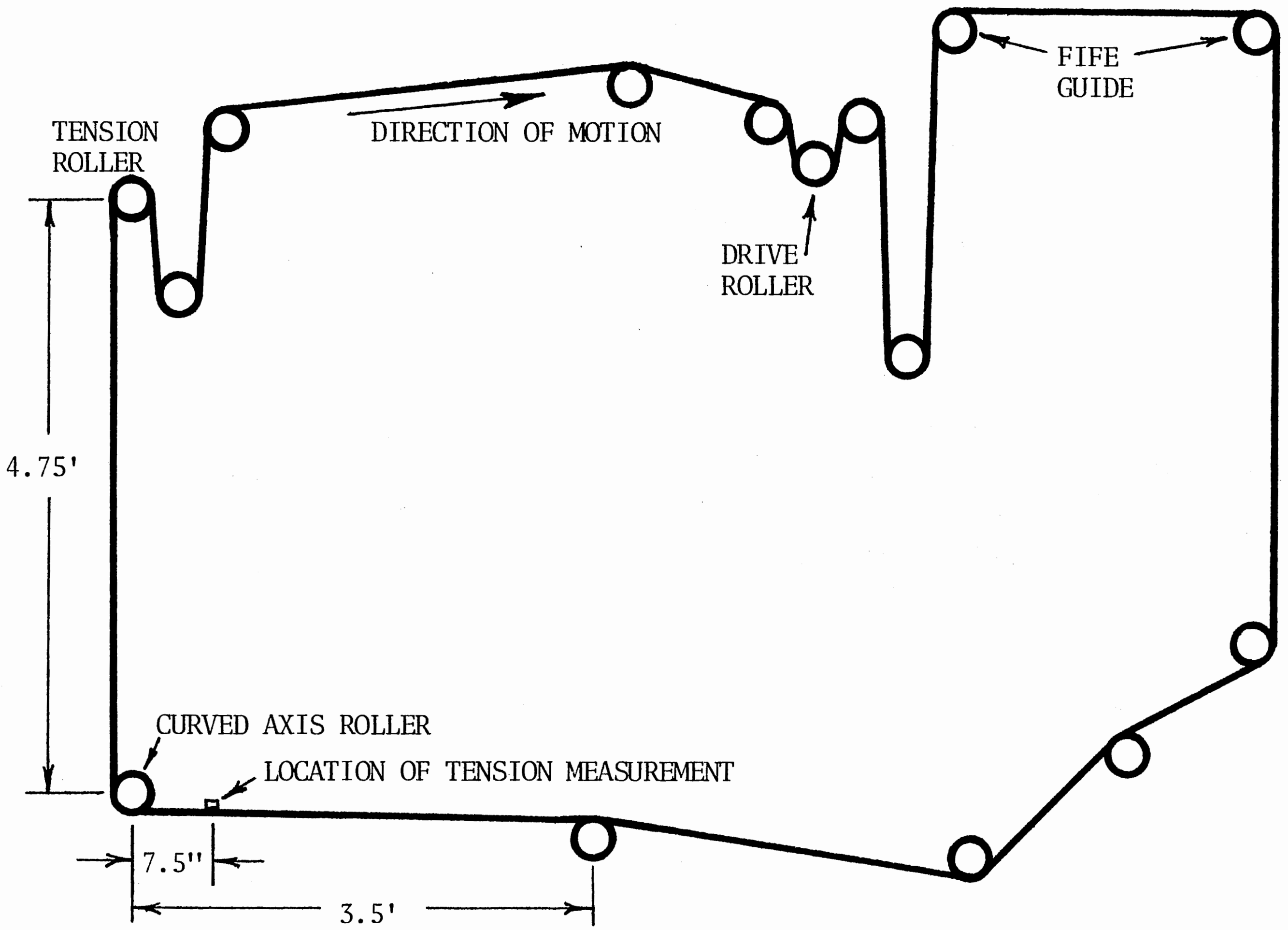

Figure 15. Web Configuration on Dynamic Machine

the roller 90 degrees. The roller was cleaned with methyl ethyl ketone prior to the testing. The roller used was a Fife "Spread Master" with a diameter of 3.5 inches and a radius of curvature of 500 inches.

CHAPTER III

RESULTS

Experimental

Static Testing

The data from the static tests verified that the transducer will work for biaxial tension measurement. The fringe patterns from the vacuum ring are concentric circles indicating uniform deflection and slope throughout at a given radius. The maximum deflection occurs at the center of the ring. Testing shows that for most webs the maximum deflection for the vacuum ring is primarily a function of the maximum tension from either the machine or lateral direction. Figure 16 contains a plot comparing deflections if there is loading in one direction to deflections if there is equal loading in both directions. Table I is sample fringe data for the vacuum ring with various loading conditions. Table II is the calculated deflections. It can be seen from the data that once a load is applied in one direction, small loads applied in the other direction have little effect on the deflection until they approach the magnitude of the orginal load.

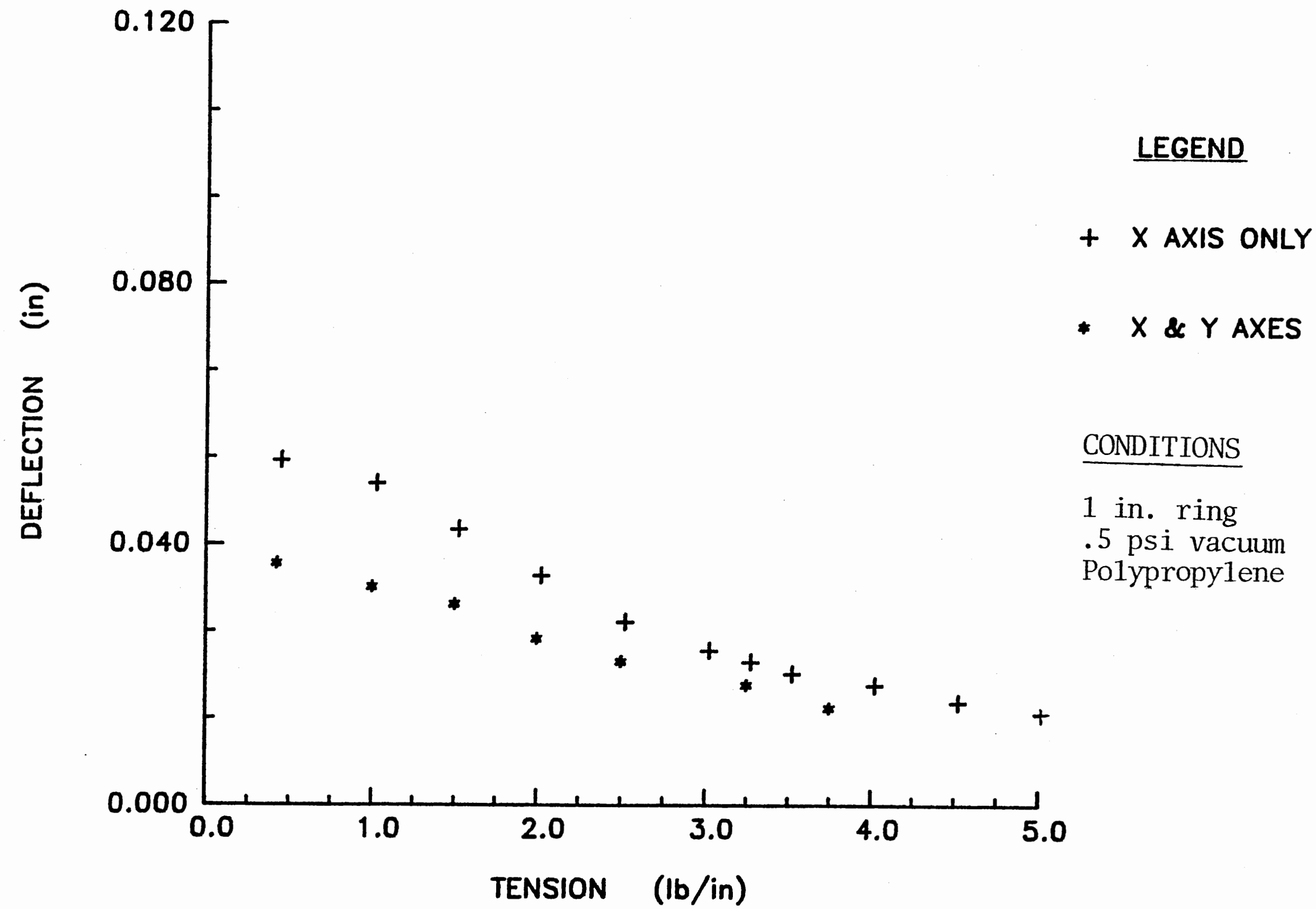

Figure 16. Comparison of Web Deflections for Uniaxial and Biaxial Loading

TABLE I

SAMPLE VACUUM RING FRINGE COUNT

Conditions

1 in. Vacuum Ring	Clear Polyester Web
1.0 psi Vacuum	Surface Painted White
Static Crucifix	Line of Sight 0.0 deg.
4 in. Wide	Light Source 45 deg.

Tension Y-Dir. lb/in	Tension X-Direction lb/in 0.42	1.00	1.50	2.00	2.50	3.00	3.50	4.00	4.50
0.00	B	6.75	6.00	5.75	5.50	5.25	5.00	4.75	4.50
0.42	6.50	6.00	5.75	5.50	5.25	5.25	5.00	4.75	4.50
1.00		5.75	5.50	5.25	5.25	5.00	4.75	4.50	4.50
1.50			5.25	5.00	5.00	4.75	4.50	4.50	4.50
2.00				5.00	4.75	4.50	4.50	4.50	4.25
2.50					4.50	-	4.25	4.25	4.00
3.00						-	4.25	4.00	3.75
3.50							4.00	3.75	3.75
4.00								-	3.50
4.50									3.50

B - Web Buckled

TABLE II

SAMPLE VACUUM RING DEFLECTION DATA

<u>Conditions</u>

1 in. Vacuum Ring	Clear Polyester Web
1.0 psi Vacuum	Surface Painted White
Static Crucifix	Line of Sight 0.0 deg.
4 in. Wide	Light Source 45 deg.

Tension Y-Dir. lb/in	Tension X-Direction lb/in								
	0.42	1.00	1.50	2.00	2.50	3.00	3.50	4.00	4.50
0.00	B	.0338	.0300	.0288	.0275	.0262	.0250	.0238	.0225
0.42	.0325	.0300	.0288	.0275	.0262	.0262	.0250	.0238	.0225
1.00		.0288	.0275	.0262	.0262	.0250	.0238	.0225	.0225
1.50			.0262	.0250	.0250	.0238	.0225	.0225	.0225
2.00				.0250	.0238	.0225	.0225	.0225	.0212
2.50					.0225	-	.0212	.0212	.0200
3.00						-	.0212	.0200	.0188
3.50							.0200	.0188	.0188
4.00								-	.0175
4.50									.0175

B - Web Buckled   1 Fringe = .005 in.

The fringe patterns for the forced displacement varied from concentric circles to concentric ellipses. The fringe patterns were circles if the tensions were the same in both directions. If the tension in the two directions differed, ellipses were formed. The shape of these ellipses is directly related to the tension in the two directions.

If the tension is known in one direction, the ellipse dimensions from the forced displacement can be used to determine the tension in the other direction. There are a couple of ways this can be done. One is to use a table of ellipse dimensions for various loading conditions. The other is to use plots of the aspect ratios of the ellipses versus a ratio of the tensions in the two directions. The aspect ratios are calculated by dividing the major axis dimension by the minor axis dimension. Table III gives sample ellipse measurements for a forced displacement. Table IV is the aspect ratio and tension ratio values for the data in Table III. Figures 17,18 and 19 are plots of aspect ratio versus tension ratio for the data given in Table IV.

The accuracy of measuring biaxial tensions can be increased by using a table of deflections for various loading conditions for the vacuum ring. This table and the ellipse tables will result in better predictions than will assuming all tension in one direction with the vacuum ring and then obtaining the other direction from

TABLE III

SAMPLE ELLIPSE DIMENSIONS FOR A FORCED DISPLACEMENT

Conditions

1 in. Diameter Hole	Clear Polyester Web
Deflection of .038 in.	Surface Painted White
Static Crucifix	Line of Sight 0.0 deg.
4 in. Wide	Light Source 45 deg.
.020 in. From Top (4th Fringe)	

Tension Y-Dir. lb/in		Tension X-Direction lb/in .42	1.0	1.5	2.0	2.5	3.0	3.5	4.0	4.5
0.00	X	B	7.9	8.0	8.1	8.2	8.3	8.4	8.4	8.5
	Y		6.0	5.6	5.3	5.1	4.9	4.8	4.5	4.3
0.42	X	7.0	7.4	7.5	7.7	7.7	8.1	8.2	8.3	8.3
	Y	6.9	6.0	5.8	5.4	5.1	4.9	4.8	4.6	4.4
1.00	X		6.8	7.0	7.1	7.2	7.4	7.5	7.6	7.6
	Y		6.2	5.9	5.7	5.4	5.1	5.0	4.8	4.5
1.50	X			6.6	6.7	6.8	7.0	7.0	7.1	7.3
	Y			6.0	5.8	5.5	5.3	5.1	4.9	4.6
2.00	X				6.5	6.5	6.6	6.7	6.8	7.0
	Y				5.9	5.6	5.4	5.2	5.0	4.7
2.50	X					6.3	-	6.4	6.4	6.7
	Y					5.7	-	5.3	5.2	4.8
3.00	X						-	6.2	6.3	6.4
	Y						-	5.3	5.3	4.9
3.50	X							6.0	6.1	6.2
	Y							5.4	5.2	4.9
4.00	X								5.8	6.0
	Y								5.2	5.0
4.50	X									5.9
	Y									5.1

B - Web Buckled   Dimensions Centimeters

TABLE IV

SAMPLE ELLIPSE ASPECT RATIO AND TENSION RATIO DATA

<u>Conditions</u>

1 in. Diameter Hole	Clear Polyester Web
Deflection of .038 in.	Surface Painted White
Static Crucifix	Line of Sight 0.0 deg.
4 in. Wide	Light Source 45 deg.
.020 in. From Top (4th Fringe)	

Tension Y-Dir. lb/in		Tension X-Direction lb/in .42	1.0	1.5	2.0	2.5	3.0	3.5	4.0	4.5
0.00	AR	B	1.32	1.43	1.53	1.61	1.69	1.75	1.87	1.98
	TR		-	-	-	-	-	-	-	-
0.42	AR	1.01	1.23	1.29	1.42	1.51	1.65	1.71	1.80	1.89
	TR	1.00	2.38	3.57	4.76	5.95	7.14	8.33	9.52	10.7
1.00	AR		1.10	1.19	1.24	1.33	1.45	1.50	1.58	1.69
	TR		1.00	1.50	2.00	2.50	3.00	3.50	4.00	4.50
1.50	AR			1.10	1.16	1.24	1.32	1.37	1.45	1.59
	TR			1.00	1.33	1.67	2.00	2.33	2.67	3.00
2.00	AR				1.10	1.16	1.22	1.29	1.36	1.49
	TR				1.00	1.25	1.50	1.75	2.00	2.25
2.50	AR					1.10	-	1.21	1.23	1.40
	TR					1.00	-	1.40	1.60	1.80
3.00	AR						-	1.17	1.19	1.31
	TR						-	1.17	1.33	1.50
3.50	AR							1.11	1.17	1.26
	TR							1.00	1.14	1.28
4.00	AR								1.12	1.20
	TR								1.00	1.12
4.50	AR									1.16
	TR									1.00

B - Web Buckled

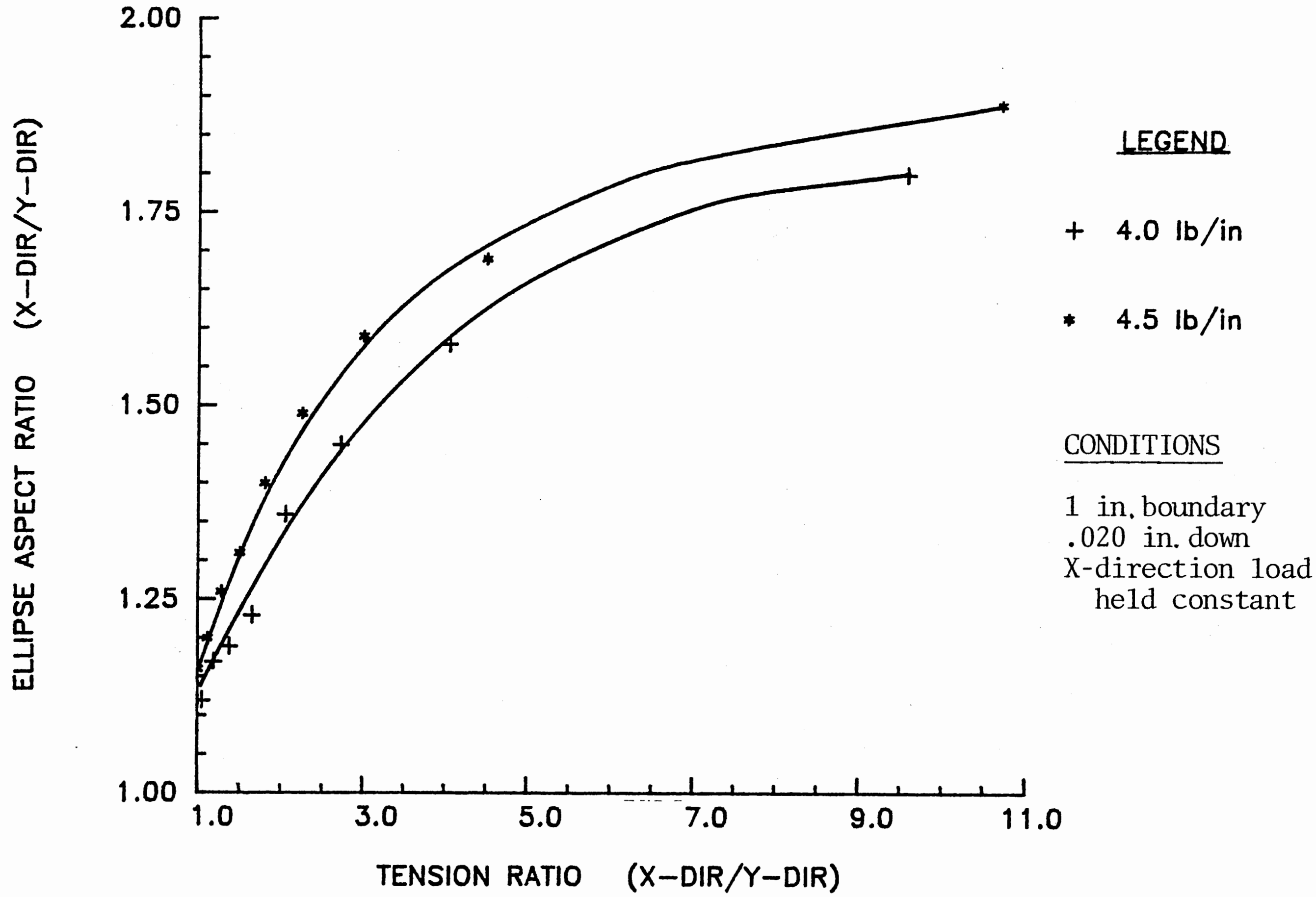

Figure 17. Ellipse Aspect Ratio vs. Tension Ratio (X-Direction Tension: 4-4.5 lb/in)

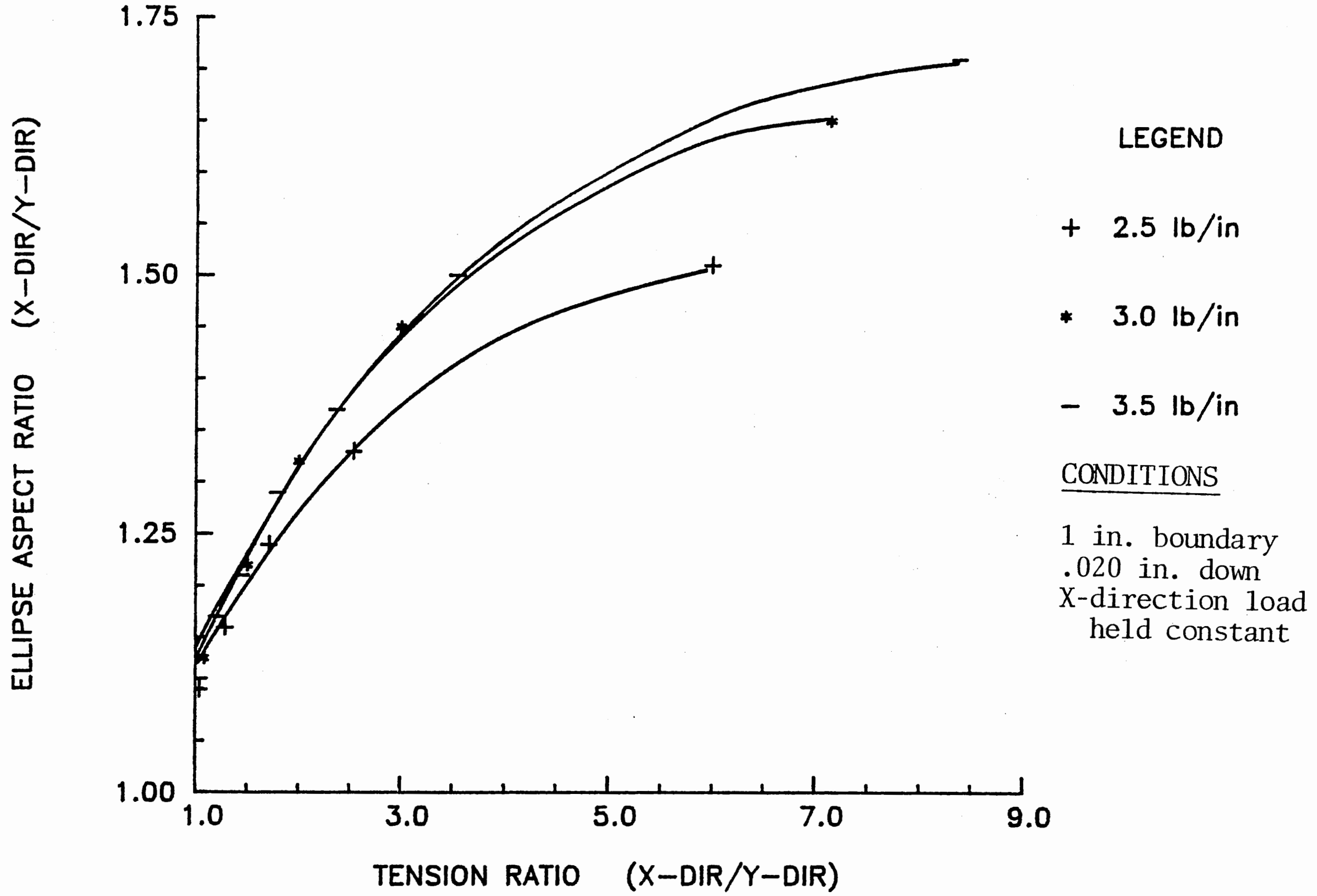

Figure 18. Ellipse Aspect Ratio vs. Tension Ratio (X-Direction Tension: 2.5-3.5 lb/in)

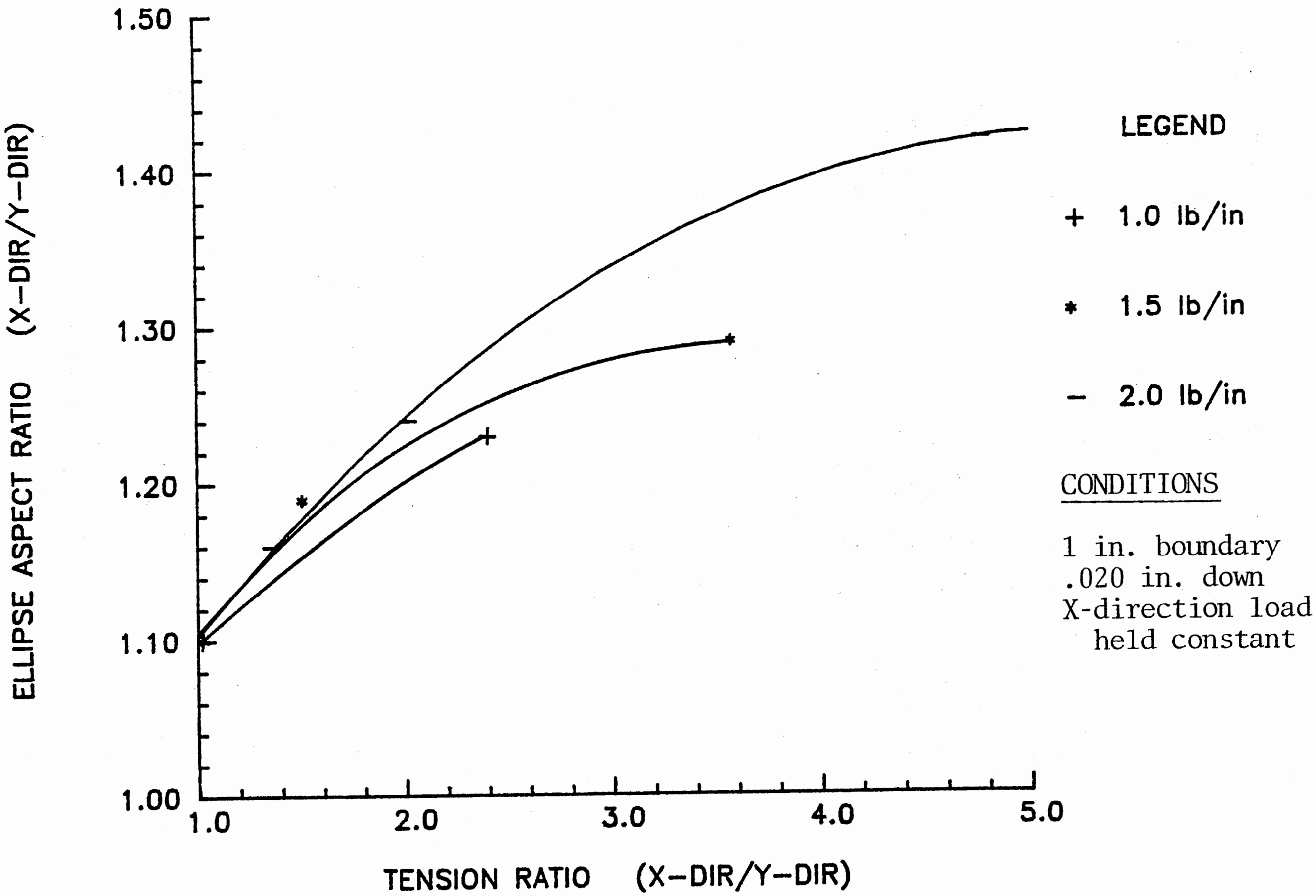

Figure 19. Ellipse Aspect Ratio vs. Tension Ratio (X-Direction Tension: 1-2 lb/in)

just the ellipse data.

The width of the web appears to have minimal effect on the vacuum ring deflection. Figure 20 is a plot of the various deflections for webs of different widths.

It is very critical that the forced displacement rod is in the center of the circular boundary plate. If the forced displacement is off center, incorrect ellipses are formed.

With the present setup the best resolution that can be obtained for measuring deflections is approximately .001 inch. This is with the light source set at 45 degrees from the vertical and the line of sight at 22.5 degrees from the vertical. If these angles are increased the resolution increases but it becomes difficult to film the fringes with the camcorder. This resolution also assumes that the fringes can be interpolated to 1/4 of a fringe.

Appendix C contains tables and plots of calibrating data for different web materials, loading conditions, and transducer configurations.

Dynamic Testing

The dynamic testing showed that the vacuum ring induced minimal friction and drag on the web. This means that accurate measurement of the web tension can be made.

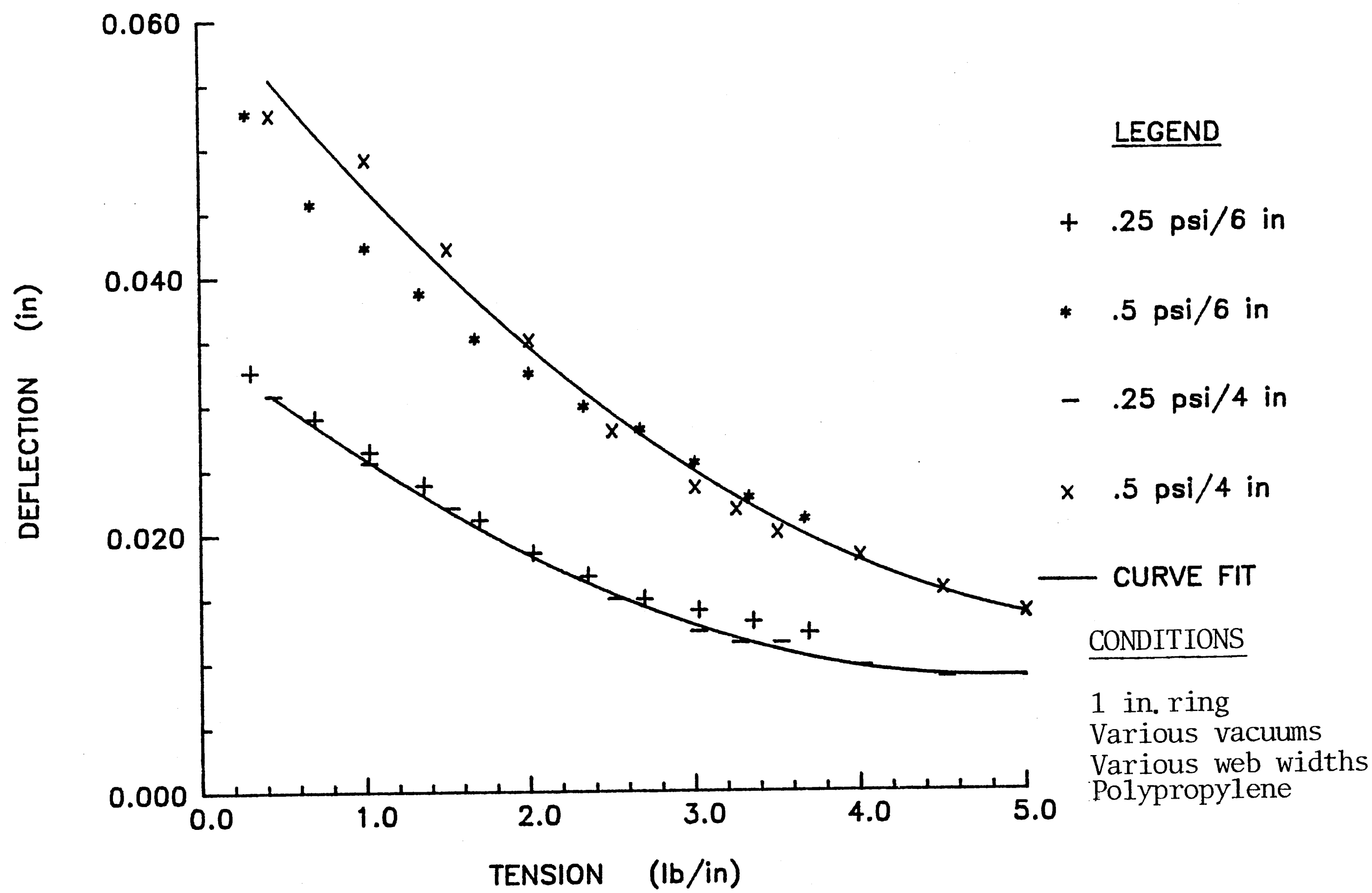

Figure 20. Effect of Web Width on Deflections

The dynamic testing, using the vacuum ring, verified that a curved axis roller causes the machine direction tension to increase in the center of the web and to decrease towards the edges. As mentioned in Chapter 2, the dynamic testing was done with the curved axis roller set in two different positions. In the first position, the bow plane is parallel to the incoming web. In the second position, the bow plane is set at a 45 degree angle below the incoming web. Figure 21 shows how the tension in the machine direction varies across the width of the web for each of the two positions of the curved axis roller. Table V gives the actual tension values across the web for both of the roller positions.

Figure 22 shows a plot of theoretical machine direction stresses and how they vary across the web width. These stresses are for a different roller and web material; but, they can be used to see that the basic behavior is the same. These theoretical stresses were computed using a finite element technique by Reynolds [6].

The testing done with the forced displacement rod verified that the curved axis roller causes the lateral tension to increase in the center of the web and decrease towards the edges. Figure 23 shows how the lateral tension varies across the width of the web for each of the two positions of the curved axis roller.

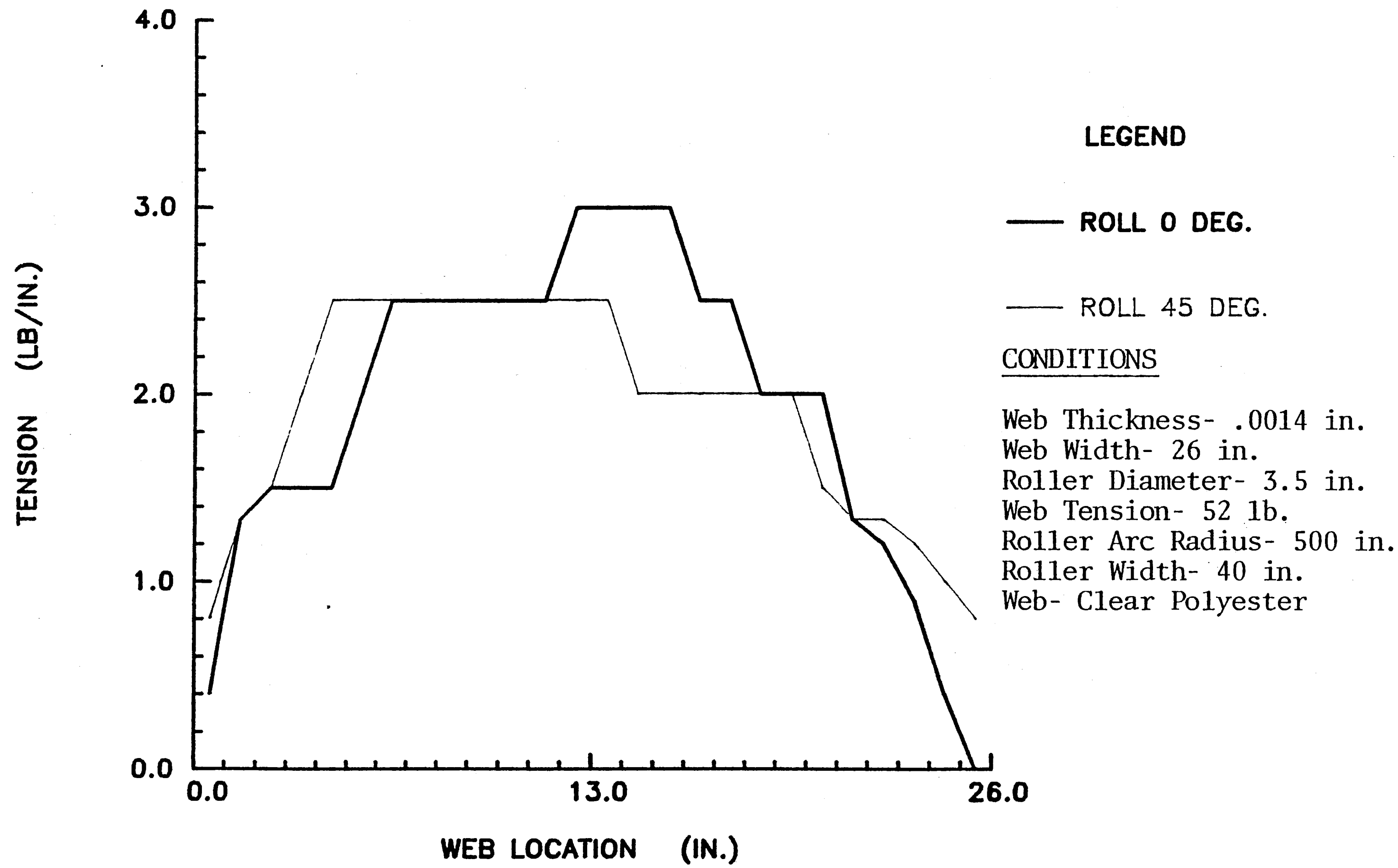

Figure 21. Curved Axis Roller Tensions in Machine Direction

TABLE V

CURVED AXIS ROLLER FRINGE DATA AND MACHINE DIRECTION TENSIONS

Conditions

1 in. Diameter Ring	Clear Polyester (1.4 mil)
1 psi Vacuum	Surface Painted White
Total Tension 52 lb.	Line of Sight 0.0 deg.
26 in. Wide	Light Source 45 deg.
Roller Diameter 3.5 in.	7.5 in. From Roller Axis
Roller Arc Radius 500 in.	Web Wraps Roll 90 deg.

Web Location (in.)	Bow Plane Parallel # Fringes	Web Tension (lb/in)	Bow Plane 45 deg. # Fringes	Web Tension (lb/in)
0.5	7.00	0.40	7.25	0.80
1.5	6.25	1.33	6.25	1.33
2.5	6.00	1.50	6.00	1.50
3.5	6.00	1.50	5.75	2.00
4.5	6.00	1.50	5.50	2.50
5.5	5.75	2.00	5.50	2.50
6.5	5.50	2.50	5.50	2.50
7.5	5.50	2.50	5.50	2.50
8.5	5.50	2.50	5.50	2.50
9.5	5.50	2.50	5.50	2.50
10.5	5.50	2.50	5.50	2.50
11.5	5.50	2.50	5.50	2.50
12.5	5.25	3.00	5.50	2.50
13.5	5.25	3.00	5.50	2.50
14.5	5.25	3.00	5.75	2.00
15.5	5.25	3.00	5.75	2.00
16.5	5.50	2.50	5.75	2.00
17.5	5.50	2.50	5.75	2.00
18.5	5.75	2.00	5.75	2.00
19.5	5.75	2.00	5.75	2.00
20.5	5.75	2.00	6.00	1.50
21.5	6.25	1.33	6.25	1.33
22.5	6.50	1.20	6.25	1.33
23.5	7.00	0.90	6.50	1.20
24.5	7.50	0.40	6.75	1.00
25.5	8.00	0.00	7.25	0.80

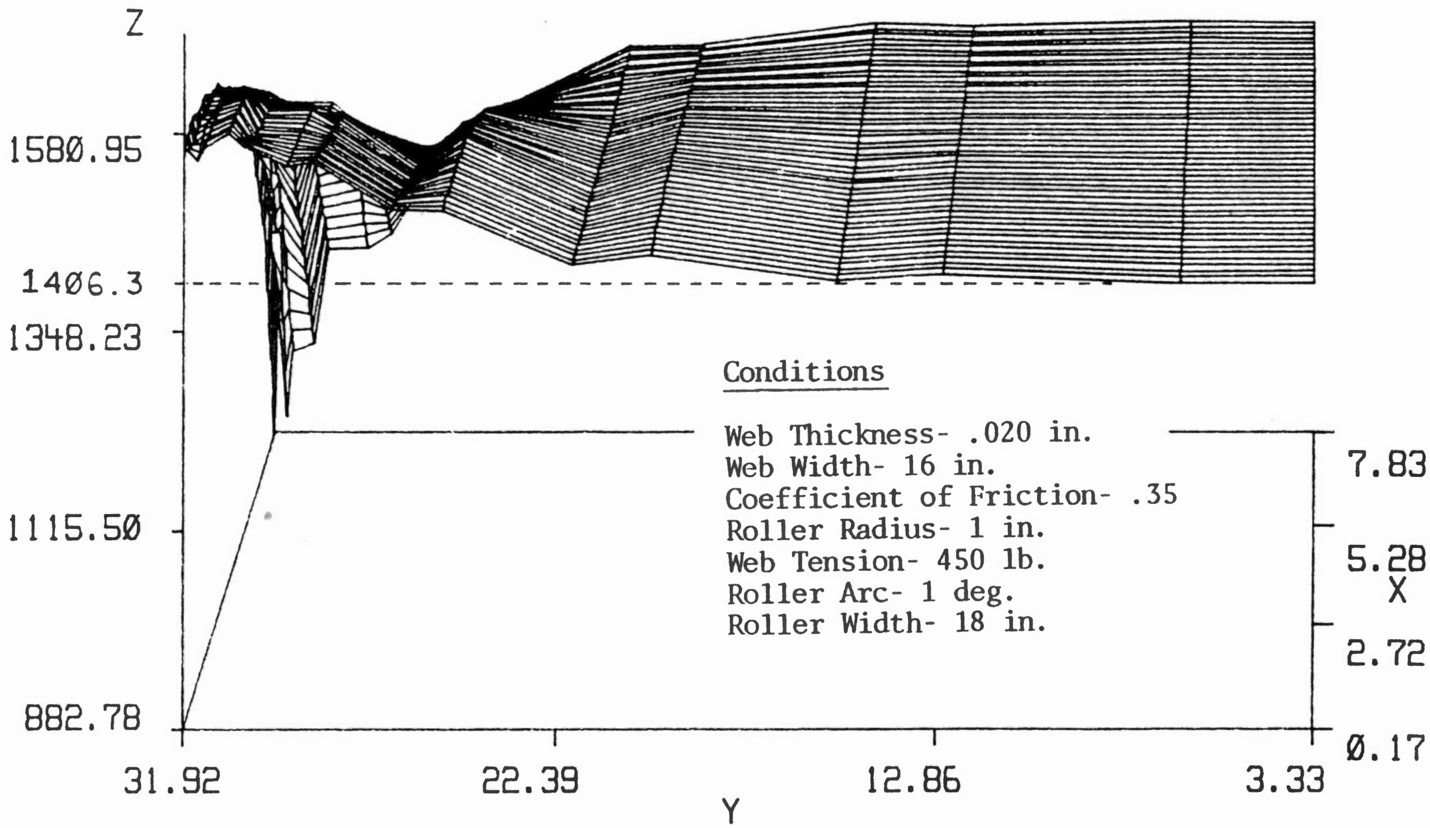

Figure 22. Theoretical Machine Direction Stresses

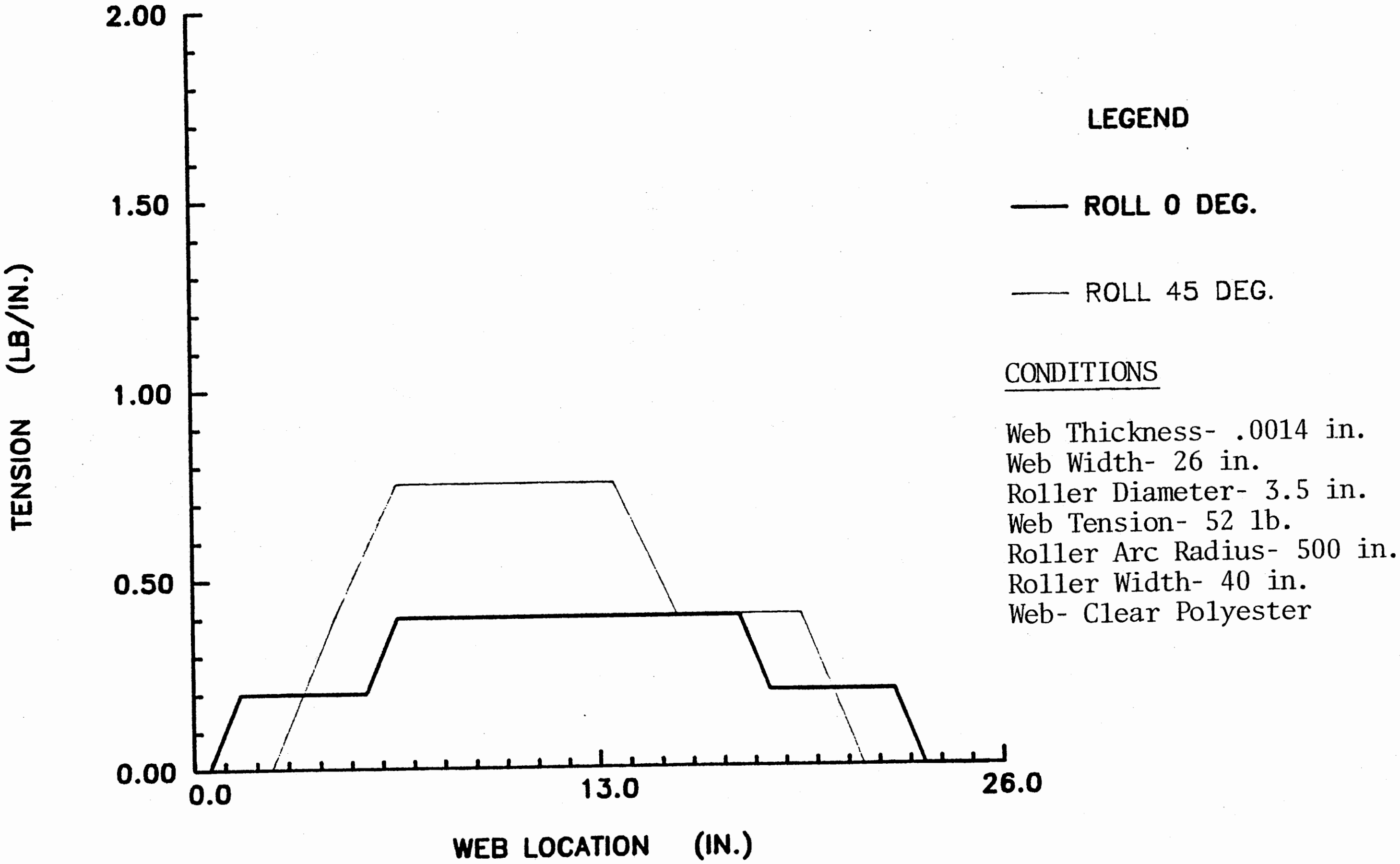

Figure 23. Curved Axis Roller Tensions in Lateral Direction

Table VI gives the lateral tension values for both of the roller positions. Due to the difficulty in calibrating the transducer at such low lateral tensions, these values are approximate.

Figure 24 shows a plot of theoretical lateral stresses and how they vary across the web width [6]. Again, these stresses are for a different roller and web material; but, they can be used to see that the basic behavior is the same.

Theoretical

The web deflection inside the vacuum ring can be closely approximated using the following equation derived from the governing equation found in Rivello [7].

$$w = Pr^2/2T_x$$

where

w = maximum out-of-plane displacement

P = pressure (vacuum)

r = radius of ring

T_x = tension in one direction

The derivation of this equation is found in Appendix D. This equation assumes tension in one direction only. A plot of this equation compared to actual deflections is in Figure 25.

TABLE VI

CURVED AXIS ROLLER ELLIPSE DATA AND LATERAL TENSIONS

Conditions

1 in. Diameter Hole	Clear Polyester (1.4 mil)
Deflection of .038 in.	Surface Painted White
Total Tension 52 lb.	Line of Sight 0.0 deg.
26 in. Wide	Light Source 45 deg.
Roller Diameter 3.5 in.	7.5 in. From Roller Axis
Roller Arc Radius 500 in.	Web Wraps Roll 90 deg.
.020 in. From Top (4th Fringe)	

Web Location (in.)	Bow Plane Parallel Web Aspect Ratio	Tension* (lb/in)	Bow Plane 45 deg. Web Aspect Ratio	Tension* (lb/in)
0.5	B	0.00	2.00	0.00
1.5	1.07	0.20		
2.5	1.15	0.20	1.56	0.00
3.5	1.25	0.20		
4.5	1.36	0.20	1.56	0.40
5.5	1.50	0.20		
6.5	1.50	0.40	1.44	0.75
7.5	1.50	0.40		
8.5	1.67	0.40	1.44	0.75
9.5	1.67	0.40		
10.5	1.67	0.40	1.44	0.75
11.5	1.67	0.40		
12.5	1.67	0.40	1.44	0.75
13.5	1.67	0.40	1.44	0.75
14.5	1.67	0.40		
15.5	1.67	0.40	1.44	0.40
16.5	1.50	0.40		
17.5	1.50	0.40	1.44	0.40
18.5	1.50	0.20		
19.5	1.50	0.20	1.44	0.40
20.5	1.36	0.20		
21.5	1.25	0.20	1.56	0.00
22.5	1.15	0.20		
23.5	1.07	0.00	1.56	0.00
24.5	1.00	0.00		
25.5	B	0.00	2.00	0.00

B - Web Buckled

* - The tensions in this table are approximate due to difficulty in calibrating the transducer at such low lateral tensions.

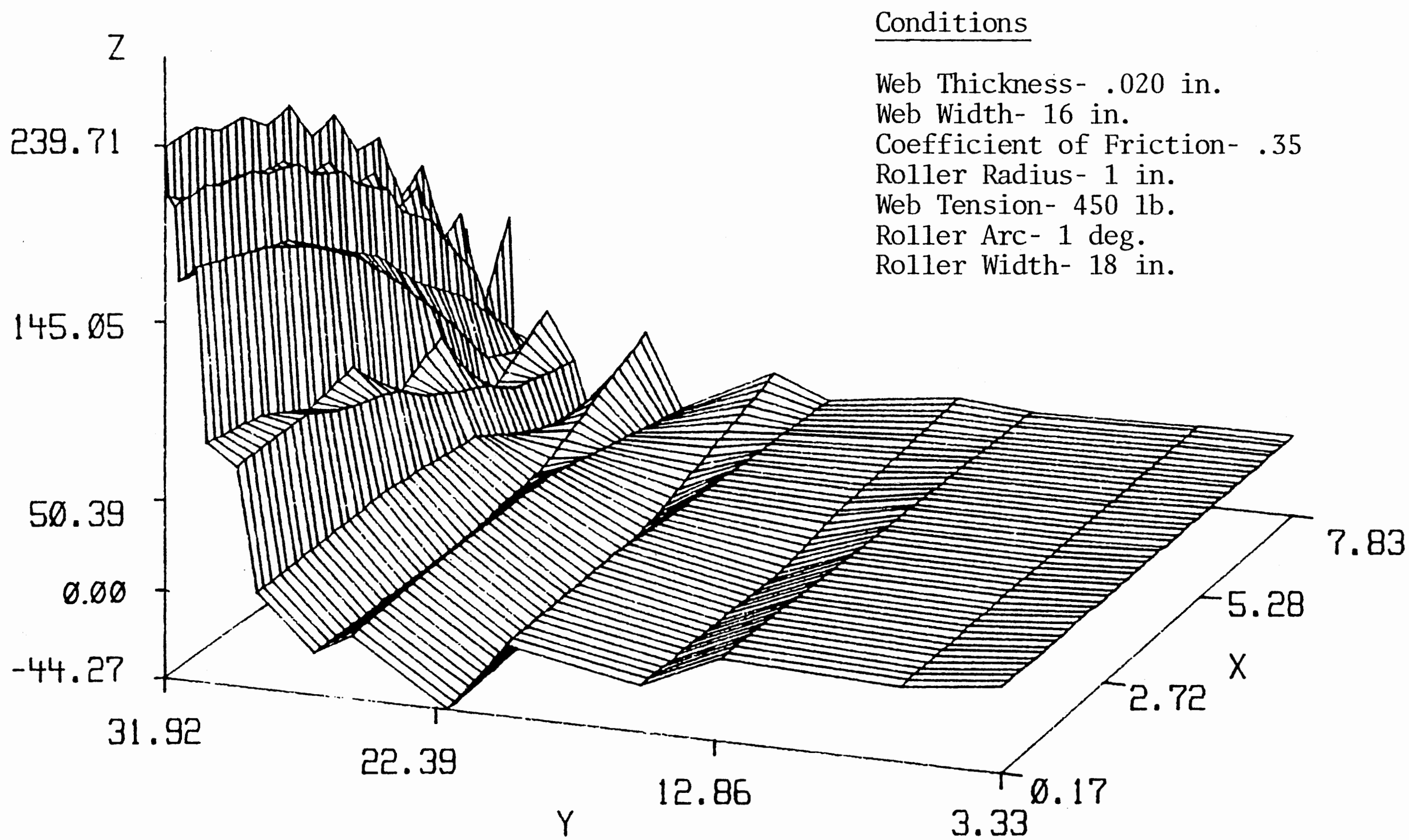

Figure 24. Theoretical Lateral Direction Stresses

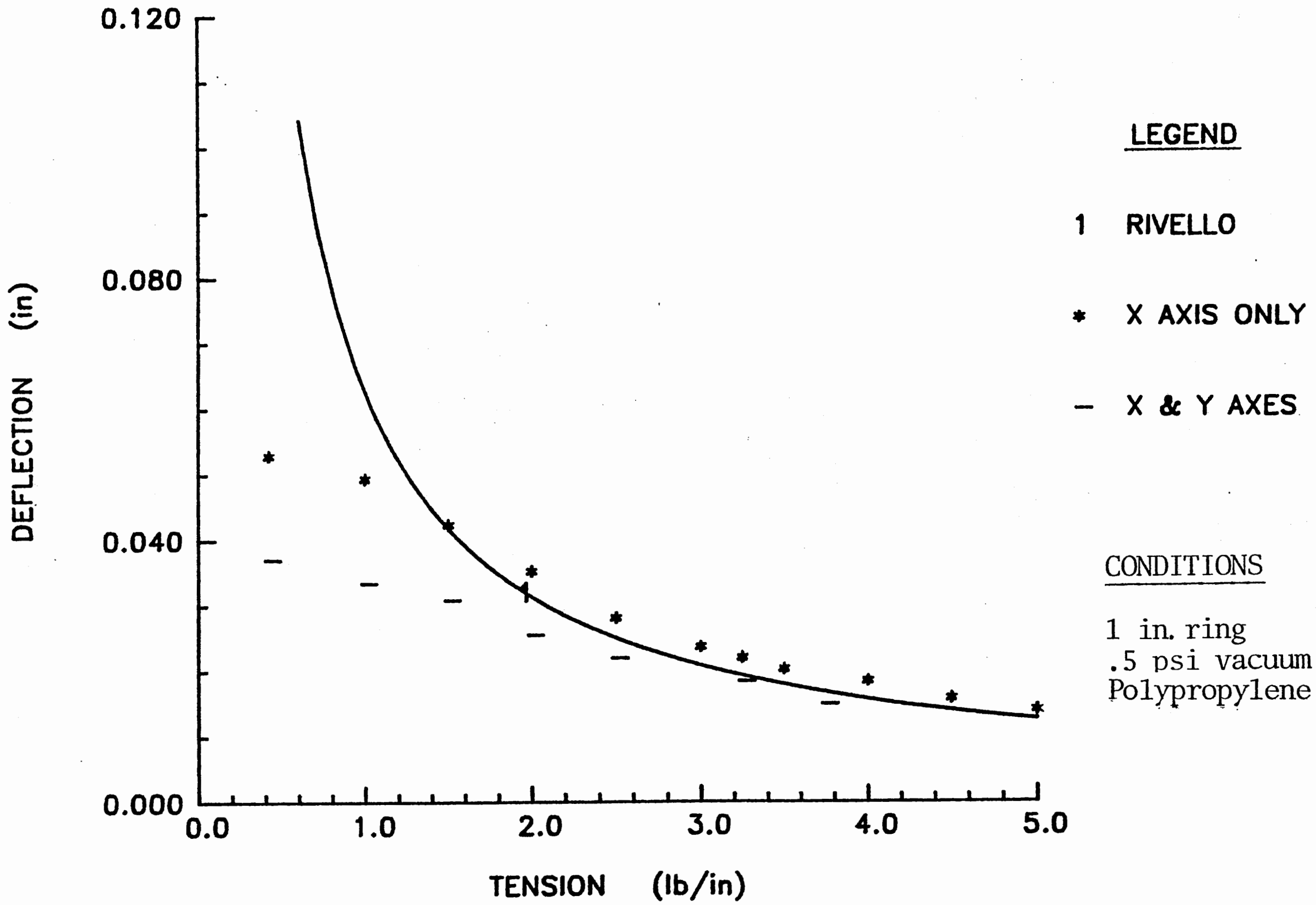

Figure 25. Comparison of Theoretical Deflection Values to Actual Values

The following assumptions were made in deriving this equation.

1. The web is perfectly flexible and is so thin that it does not offer any resistance to bending. It is only capable of resisting tension.

2. Deflections are large, many times greater than the web thickness.

3. Lateral pressure (vacuum) causes no appreciable change in the web tension.

4. The equation is independent of web material properties. It is a pure equalibrium equation.

5. The boundary condition is a roller support all along the edge.

The variation in the experimental and theoretical results can be accounted for for the following reasons.

1. The web does offer a slight resistance to bending. This is particularly noticeable at low pressures (vacuum).

2. The boundary condition is not a pure roller and causes a closed boundary effect.

3. The configuration of the actual applied tensions are not as assumed in the equation derivation.

4. The deflection is affected by the web's thickness and material properties.

5. Error in experimental measurement.

CHAPTER IV

CONCLUSIONS

Overview

The web biaxial stress transducer performs as intended and has all the capabilities needed. The present transducer is capable of measuring biaxial tension to within .5 pounds per inch or better. This resolution is adequate for most applications. The transducer can be used to measure uniaxial tension with resolution better than .5 pounds per inch if there is no lateral tension and if extremely accurate calibrating techniques are used. (As an example the resolution could be increased to .2 pounds per inch if a grating with 1000 lines per inch were used and it was calibrated with a load cell.) With proper development, the transducer and its principles could be adapted for industrial use and its accuracy improved.

Recommendations

In the event of further study or development of this transducer the following recommendations are made:

1. The forced displacement rod and circular

boundary plate need to be modified to handle dynamic measurements.

2. A good method for reading fringe patterns on clear and reflective type webs needs to be developed.

3. A digital, electronic type recording device would greatly increase the efficiency of reading the fringe patterns.

4. A moire' grating with a greater pitch would increase the number of fringes and consequently the accuracy of the deflection measurements.

5. Other techniques including laser reflection (e.g optical arm) or fiber optics measurement of the web deflection should be considered.

6. The transducer frame could be modified to allow measurement closer to a curved axis roller.

LITERATURE CITED

1. Bak, David J. "Dancer Arm Feedback Regulates Tension Control" Design News, 43, 6 April 1987, pp. 132-133.

2. Dally, James W., and William F. Riley. Experimental Stress Analysis. Ed. B.J. Clark and Madelaine Eichberg. 2nd ed. New York: McGraw-Hill Inc., 1978.

3. Hansen, Age. "A Portable Instrument for Web-Tension Control and Cross-Profile Recording" Tappi Journal, 69, December 1986, pp. 48-51.

4. Larsson, L.O., ed. Advances and Trends in Winding Technology. Djursholm, Sweden: Swedish Newsprint Research Centre (TFL), 1987.

5. Nutter, Darin W. "Investigation of Experimental Noncontact Tension Methods." Master's thesis, Oklahoma State University, 1988.

6. Reynolds, Brett Harrison. "Stress Distribution Computation Within a Membrane Due to a Curved-Axis Roller." Master's thesis, Oklahoma State University, 1986.

7. Rivello, Robert M. Theory and Analysis of Flight Structures. New York: McGraw-Hill Inc., 1969.

8. Satas, Donatas, ed. Web Processing and Converting Technology and Equipment. Van Nos Reinhold, 1984.

9. Theocaris, Pericles S. Moire' Fringes in Strain Analysis. Oxford, New York: Pergamon Press, 1969.

10. Timoshenko, S. Theory of Plates and Shells. 2nd ed. New York: McGraw-Hill Inc., 1959.

11. Ugural, A.C. Stresses in Plates and Shells. Ed. Frank J. Cerra. New York: McGraw-Hill Inc., 1981.

APPENDIXES

APPENDIX A

EFFECT OF RING OR PLATE AND GRATING NOT BEING PARALLEL

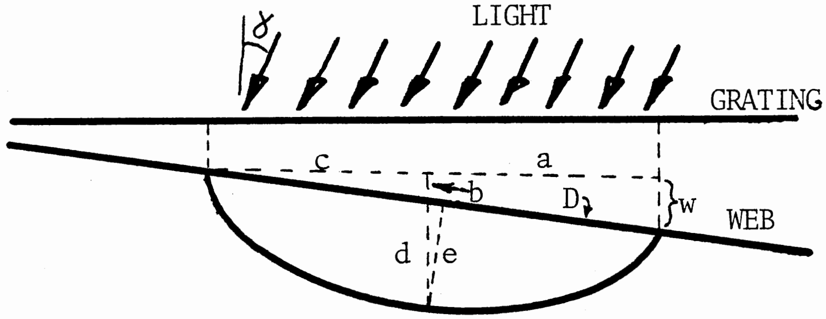

Figure 26. Ring and Grating not Parallel

Calculations

Assume
γ = angle of light = 45 deg.

p = pitch of the master grating = 1/200 in.

n = order of the moire' fringe = 3 (across diameter)

D = ring diameter = 1.5 in.

c is measured

Find deflection w
$w = np/\tan\gamma$

$w = n(.005)$

$w = (3)(.005)$

w = .015 in

By Pythagorean's Theorem
$a+c = \sqrt{D^2 - w^2}$

$a+c = \sqrt{1.50^2 - .015^2}$

a+c = 1.499925 in.

By similiar triangles
$e/d = a+c/D$

$e/d = 1.4999/1.5$ ***

For small angles the difference between e and d is very small; therefore, compensation for small angles can be neglected.

APPENDIX B

CALCULATING OUT-OF-PLANE DISPLACEMENTS IF THE LINE OF SIGHT IS NOT VERTICAL

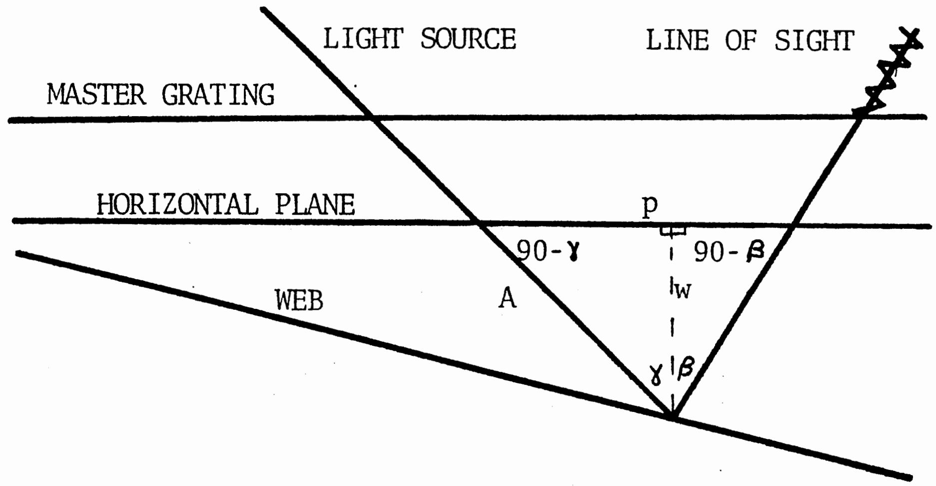

Figure 27. Line of Sight not Vertical

<u>Calculations</u>
Refer to Figures 9 and 27.

Law of Sines

$\sin(\gamma+\beta)/p = \sin(90-\beta)/A$ $\qquad$ $w/A = \cos\gamma$

$\sin(\gamma+\beta)/p = \cos\beta/(w/\cos\gamma)$ $\qquad$ $A = w/\cos\gamma$

$\sin(\gamma+\beta)/p = \cos\beta\cos\gamma/w$

$p/\sin(\gamma+\beta) = w/\cos\beta\cos\gamma$

$w = p(\cos\beta\cos\gamma)/\sin(\gamma+\beta)$

For the case of "n" fringes.

$w = np(\cos\beta\cos\gamma)/\sin(\gamma+\beta)$

For the case of vertical line of sight ($\beta = 0$)

$w = p/\tan\gamma$ and $w = np/\tan\gamma$

APPENDIX C

DATA FROM STATIC TESTING

TABLE VII

VACUUM RING FRINGE COUNT DATA
(TEST #1)

<u>Conditions</u>

1 in. Vacuum Ring
.25 psi Vacuum
Static Crucifix
4 in. Wide

Polypropylene Web
Line of Sight 22.5 deg.
Light Source 45 deg.

Tension Y-Dir. lb/in	Tension X-Direction lb/in							
	0.42	1.00	1.50	2.00	2.50	3.00	3.25	3.75
0.00	9.25	8.25	7.25	6.25	5.25	4.25	4.25	3.25
0.42	8.50	8.25	7.50	6.50	5.75	4.75	4.50	3.25
1.00		7.25	7.00	6.75	6.25	5.25	4.25	3.50
1.50			6.25	5.75	5.50	5.25	4.25	3.50
2.00				5.00	4.75	4.50	4.00	3.50
2.50					4.25	-	3.50	3.25
3.25							3.00	2.75
3.75								2.50

TABLE VIII

VACUUM RING DEFLECTION DATA
(TEST #1)

<u>Conditions</u>

1 in. Vacuum Ring
.25 psi Vacuum
Static Crucifix
4 in. Wide

Polypropylene Web
Line of Sight 22.5 deg.
Light Source 45 deg.

Tension Y-Dir. lb/in	Tension X-Direction lb/in							
	0.42	1.00	1.50	2.00	2.50	3.00	3.25	3.75
0.00	.0372	.0291	.0256	.0221	.0185	.0150	.0150	.0115
0.42	.0300	.0291	.0256	.0229	.0203	.0168	.0159	.0115
1.00		.0256	.0247	.0238	.0221	.0185	.0150	.0124
1.50			.0221	.0203	.0194	.0185	.0150	.0124
2.00				.0176	.0168	.0159	.0141	.0124
2.50					.0150	-	.0124	.0115
3.25							.0106	.0097
3.75								.0088

1 Fringe = .00353 in.

TABLE IX

VACUUM RING FRINGE COUNT DATA
(TEST #2)

<u>Conditions</u>

1 in. Vacuum Ring	Polypropylene Web
.50 psi Vacuum	Line of Sight 22.5 deg.
Static Crucifix	Light Source 45 deg.
4 in. Wide	

Tension Y-Dir. lb/in	Tension X-Direction lb/in 0.42	1.00	1.50	2.00	2.50	3.00	3.25	3.75
0.00	11.0	10.0	9.25	8.50	7.50	6.50	6.00	5.25
0.42	10.5	10.0	9.50	8.75	7.75	6.75	6.25	5.50
1.00		9.50	9.25	8.75	8.25	7.25	6.75	6.25
1.50			8.75	8.25	7.75	7.25	7.00	6.00
2.00				7.25	7.00	6.50	6.50	6.00
2.50					6.25	-	5.75	5.50
3.25							5.25	4.50
3.75								4.25

TABLE X

VACUUM RING DEFLECTION DATA
(TEST #2)

<u>Conditions</u>

1 in. Vacuum Ring
.50 psi Vacuum
Static Crucifix
4 in. Wide

Polypropylene Web
Line of Sight 22.5 deg.
Light Source 45 deg.

Tension Y-Dir. lb/in	Tension X-Direction lb/in							
	0.42	1.00	1.50	2.00	2.50	3.00	3.25	3.75
0.00	.0388	.0353	.0326	.0300	.0265	.0229	.0212	.0185
0.42	.0371	.0353	.0335	.0309	.0274	.0238	.0221	.0194
1.00		.0335	.0326	.0309	.0291	.0256	.0238	.0221
1.50			.0309	.0291	.0274	.0256	.0247	.0212
2.00				.0256	.0247	.0229	.0229	.0212
2.50					.0221	-	.0203	.0194
3.25							.0185	.0159
3.75								.0150

1 Fringe = .00353 in.

TABLE XI

ELLIPSE DIMENSIONS FOR A FORCED DISPLACEMENT (TEST #3)

Conditions

1 in. Diameter Hole	Clear Polyester Web
Deflection of .038 in.	Surface Painted White
Static Crucifix	Line of Sight 0.0 deg.
4 in. Wide	Light Source 45 deg.
.015 in. From Top (3rd Fringe)	

Tension Y-Dir. lb/in		Tension X-Direction lb/in .42	1.0	1.5	2.0	2.5	3.0	3.5	4.0	4.5
0.00	X	B	5.3	5.3	5.4	5.4	5.5	5.5	5.6	5.7
	Y		4.0	3.7	3.5	3.3	3.2	3.1	3.0	2.9
0.42	X	4.6	4.8	5.0	5.0	5.0	5.3	5.4	5.5	5.6
	Y	4.6	4.0	3.8	3.6	3.4	3.3	3.2	3.1	3.0
1.00	X		4.4	4.5	4.6	4.7	4.8	4.8	5.0	5.0
	Y		4.2	3.9	3.7	3.5	3.4	3.3	3.2	3.0
1.50	X			4.2	4.3	4.5	4.5	4.5	4.6	4.7
	Y			4.0	3.8	3.6	3.4	3.3	3.2	3.0
2.00	X				4.1	4.2	4.2	4.3	4.3	4.5
	Y				3.9	3.7	3.6	3.4	3.3	3.1
2.50	X					4.0	-	4.1	4.2	4.3
	Y					3.7	-	3.4	3.3	3.1
3.00	X						-	3.9	4.0	4.1
	Y						-	3.5	3.3	3.1
3.50	X							3.6	3.9	3.9
	Y							3.5	3.4	3.2
4.00	X								3.7	3.8
	Y								3.4	3.3
4.50	X									3.6
	Y									3.3

B - Web Buckled Dimensions Centimeters

TABLE XII

ELLIPSE ASPECT RATIO AND TENSION RATIO DATA (TEST #3)

Conditions

1 in. Diameter Hole
Deflection of .038 in.
Static Crucifix
4 in. Wide
.015 in. From Top (3rd Fringe)

Clear Polyester Web
Surface Painted White
Line of Sight 0.0 deg.
Light Source 45 deg.

Tension Y-Dir. lb/in		Tension X-Direction lb/in: .42	1.0	1.5	2.0	2.5	3.0	3.5	4.0	4.5
0.00	AR	B	1.32	1.43	1.54	1.64	1.72	1.77	1.87	1.96
	TR		-	-	-	-	-	-	-	-
0.42	AR	1.00	1.20	1.32	1.39	1.47	1.61	1.67	1.77	1.87
	TR	1.00	2.38	3.57	4.76	5.95	7.14	8.33	9.52	10.7
1.00	AR		1.05	1.15	1.24	1.34	1.41	1.45	1.56	1.67
	TR		1.00	1.50	2.00	2.50	3.00	3.50	4.00	4.50
1.50	AR			1.05	1.13	1.25	1.32	1.36	1.44	1.57
	TR			1.00	1.33	1.67	2.00	2.33	2.67	3.00
2.00	AR				1.05	1.14	1.17	1.26	1.30	1.45
	TR				1.00	1.25	1.50	1.75	2.00	2.25
2.50	AR					1.08	-	1.20	1.27	1.39
	TR					1.00	-	1.40	1.60	1.80
3.00	AR						-	1.11	1.21	1.32
	TR						-	1.17	1.33	1.50
3.50	AR							1.06	1.15	1.22
	TR							1.00	1.14	1.28
4.00	AR								1.09	1.15
	TR								1.00	1.12
4.50	AR									1.09
	TR									1.00

B - Web Buckled

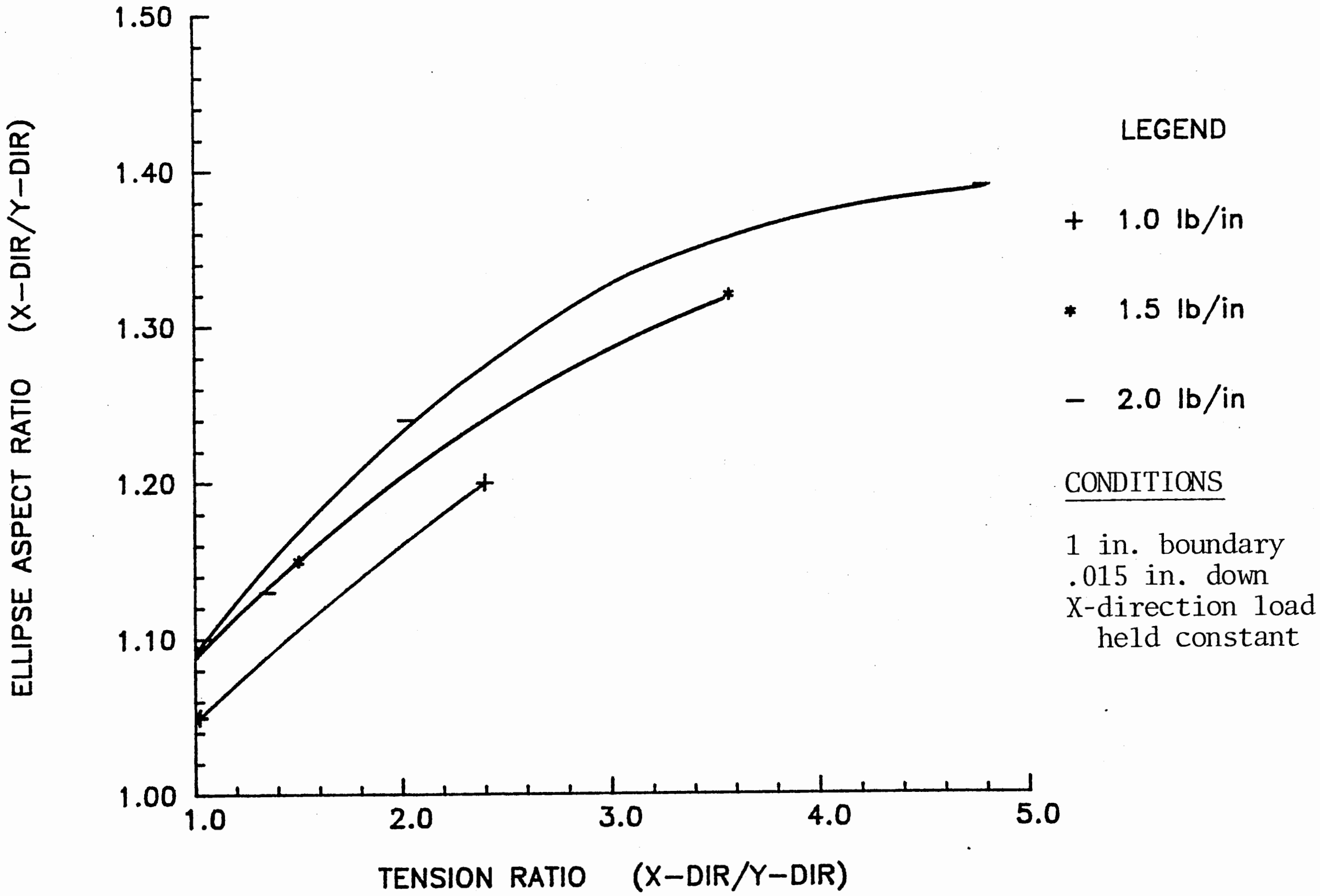

Figure 28. Test #3: Ellipse Aspect Ratio vs. Tension Ratio (X-Direction Tension: 1-2 lb/in)

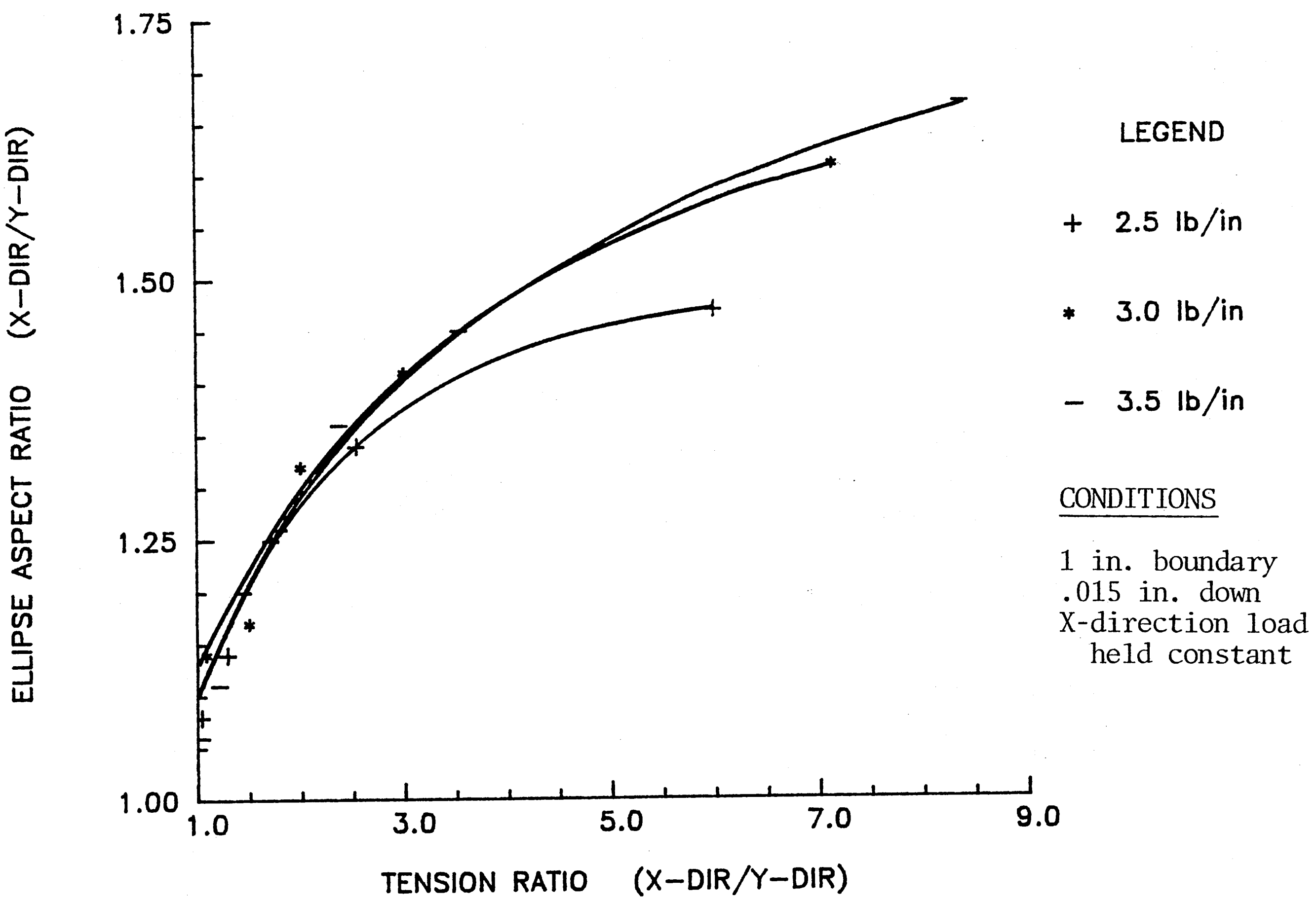

Figure 29. Test #3: Ellipse Aspect Ratio vs. Tension Ratio (X-Direction Tension: 2.5-3.5 lb/in)

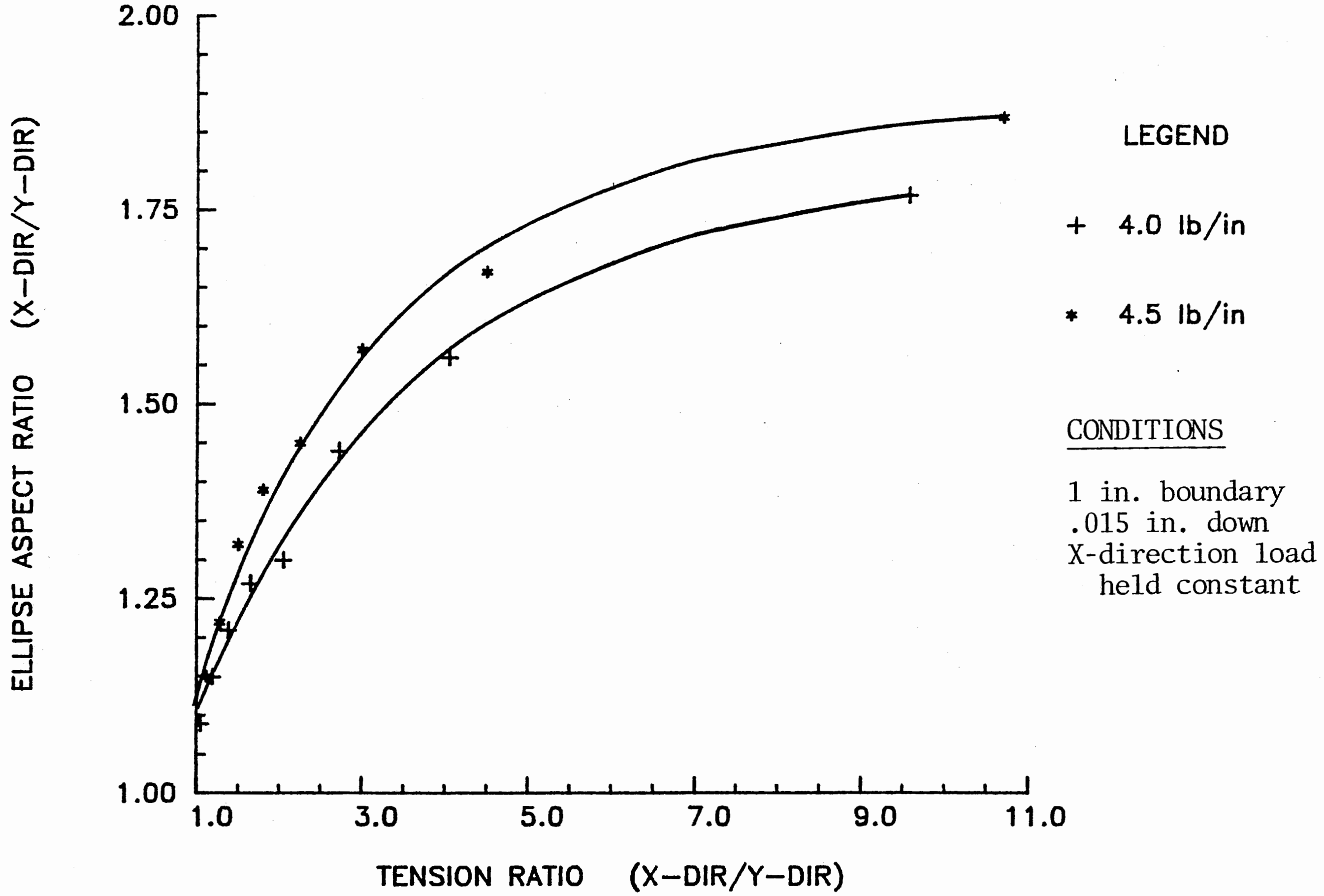

Figure 30. Test #3: Ellipse Aspect Ratio vs. Tension Ratio (X-Direction Tension: 4-4.5 lb/in)

TABLE XIII

ELLIPSE DIMENSIONS FOR A FORCED DISPLACEMENT (TEST #4)

Conditions

1 in. Diameter Hole
Deflection of .038 in.
Static Crucifix
4 in. Wide
.021 in. From Top (3rd Fringe)

Clear Polyester Web
Surface Painted White
Line of Sight 0.0 deg.
Light Source 35 deg.

Tension Y-Dir. lb/in		Tension X-Direction lb/in .42	1.0	1.5	2.0	2.5	3.0	3.5	4.0	4.5
0.00	X	B	7.2	7.3	7.3	7.5	7.7	7.7	7.7	7.8
	Y		5.5	5.1	4.8	4.7	4.3	4.2	4.2	4.0
0.42	X	6.5	6.7	6.7	6.9	7.1	7.3	7.3	7.4	7.5
	Y	6.2	5.7	5.2	4.9	4.7	4.4	4.4	4.2	4.0
1.00	X		6.0	6.2	6.3	6.6	6.6	6.7	6.8	7.0
	Y		5.8	5.3	5.1	4.8	4.6	4.4	4.3	4.1
1.50	X			6.0	5.9	6.1	6.4	6.2	6.4	6.5
	Y			5.5	5.1	4.9	4.7	4.6	4.4	4.2
2.00	X				5.8	5.9	6.0	-	6.1	6.2
	Y				5.2	4.9	4.7	-	4.5	4.2
2.50	X					5.6	-	-	5.9	6.0
	Y					5.0	-	-	4.5	4.4
3.00	X						-	-	5.6	5.8
	Y						-	-	4.6	4.4
3.50	X							5.4	5.4	5.5
	Y							4.7	4.6	4.5
4.00	X								5.3	5.4
	Y								4.6	4.5
4.50	X									5.2
	Y									4.5

B - Web Buckled

Dimensions Centimeters

TABLE XIV

ELLIPSE ASPECT RATIO AND TENSION RATIO DATA (TEST #4)

Conditions

1 in. Diameter Hole	Clear Polyester Web
Deflection of .038 in.	Surface Painted White
Static Crucifix	Line of Sight 0.0 deg.
4 in. Wide	Light Source 35 deg.
.021 in. From Top (3rd Fringe)	

Tension Y-Dir. lb/in		Tension X-Direction lb/in .42	1.0	1.5	2.0	2.5	3.0	3.5	4.0	4.5
0.00	AR	B	1.31	1.43	1.52	1.60	1.79	1.83	1.83	1.95
	TR		-	-	-	-	-	-	-	-
0.42	AR	1.05	1.18	1.28	1.41	1.51	1.66	1.66	1.76	1.88
	TR	1.00	2.38	3.57	4.76	5.95	7.14	8.33	9.52	10.7
1.00	AR		1.03	1.17	1.24	1.38	1.43	1.52	1.58	1.71
	TR		1.00	1.50	2.00	2.50	3.00	3.50	4.00	4.50
1.50	AR			1.09	1.16	1.24	1.36	1.35	1.45	1.55
	TR			1.00	1.33	1.67	2.00	2.33	2.67	3.00
2.00	AR				1.12	1.20	1.28	-	1.36	1.48
	TR				1.00	1.25	1.50	-	2.00	2.25
2.50	AR					1.12	-	-	1.31	1.36
	TR					1.00	-	-	1.60	1.80
3.00	AR						-	-	1.22	1.32
	TR						-	-	1.33	1.50
3.50	AR							1.15	1.17	1.22
	TR							1.00	1.14	1.28
4.00	AR								1.15	1.20
	TR								1.00	1.12
4.50	AR									1.16
	TR									1.00

B - Web Buckled

TABLE XV

ELLIPSE ASPECT RATIO AND TENSION RATIO DATA (TEST #5)

Conditions

1 in. Diameter Hole	Clear Polyester Web
Deflection of .035 in.	Surface Painted White
Static Crucifix	Line of Sight 0.0 deg.
4 in. Wide	Light Source 35 deg.
.021 in. From Top (3rd Fringe)	

Tension Y-Dir. lb/in		Tension X-Direction lb/in .42	1.0	1.5	2.0	2.5	3.0	3.5	4.0	4.5
0.00	AR	B	1.42	1.55	1.62	1.67	1.78	1.92	1.97	2.03
	TR		-	-	-	-	-	-	-	-
0.42	AR	1.03	1.19	1.30	1.40	1.55	1.65	1.70	1.79	1.97
	TR	1.00	2.38	3.57	4.76	5.95	7.14	8.33	9.52	10.7
1.00	AR		1.08	1.21	1.23	1.40	1.45	1.50	1.62	1.62
	TR		1.00	1.50	2.00	2.50	3.00	3.50	4.00	4.50
1.50	AR			1.08	1.12	1.20	1.27	1.40	1.40	1.51
	TR			1.00	1.33	1.67	2.00	2.33	2.67	3.00
2.00	AR				1.08	1.15	1.21	1.25	1.37	1.49
	TR				1.00	1.25	1.50	1.75	2.00	2.25
2.50	AR					1.07	-	-	1.30	1.38
	TR					1.00	-	-	1.60	1.80
3.00	AR						-	-	1.21	1.26
	TR						-	-	1.33	1.50
3.50	AR							1.11	1.20	-
	TR							1.00	1.14	-
4.00	AR								1.07	1.14
	TR								1.00	1.12

B - Web Buckled

TABLE XVI

ELLIPSE ASPECT RATIO AND TENSION
RATIO DATA (TEST #5)

Conditions

1 in. Diameter Hole	Clear Polyester Web
Deflection of .035 in.	Surface Painted White
Static Crucifix	Line of Sight 0.0 deg.
4 in. Wide	Light Source 35 deg.
.021 in. From Top (3rd Fringe)	

Tension Y-Dir. lb/in		Tension X-Direction lb/in .42	1.0	1.5	2.0	2.5	3.0	3.5	4.0	4.5
0.00	AR	B	1.42	1.55	1.62	1.67	1.78	1.92	1.97	2.03
	TR		-	-	-	-	-	-	-	-
0.42	AR	1.03	1.19	1.30	1.40	1.55	1.65	1.70	1.79	1.97
	TR	1.00	2.38	3.57	4.76	5.95	7.14	8.33	9.52	10.7
1.00	AR		1.08	1.21	1.23	1.40	1.45	1.50	1.62	1.62
	TR		1.00	1.50	2.00	2.50	3.00	3.50	4.00	4.50
1.50	AR			1.08	1.12	1.20	1.27	1.40	1.40	1.51
	TR			1.00	1.33	1.67	2.00	2.33	2.67	3.00
2.00	AR				1.08	1.15	1.21	1.25	1.37	1.49
	TR				1.00	1.25	1.50	1.75	2.00	2.25
2.50	AR					1.07	-	-	1.30	1.38
	TR					1.00	-	-	1.60	1.80
3.00	AR						-	-	1.21	1.26
	TR						-	-	1.33	1.50
3.50	AR							1.11	1.20	-
	TR							1.00	1.14	-
4.00	AR								1.07	1.14
	TR								1.00	1.12

B - Web Buckled

TABLE XVII

VACUUM RING FRINGE COUNT DATA
(TEST #6)

Conditions

1 in. Vacuum Ring	Clear Polyester Web
Static Crucifix	Surface Painted White
4 in. Wide	Line of Sight 0.0 deg.

		Tension X-Direction (lb/in)					
	Tension	(Light Source 35 deg.)			(Light Source 45 deg.)		
Vacuum (psi)	Y-Dir. (lb/in)	Same As Y	.42	4.5	Same As Y	.42	4.5
0.50	0.00	-	-	2.75	-	-	3.50
	0.42	4.50	4.50	2.75	7.50	7.50	3.50
	1.00	4.00	4.25	2.75	5.75	6.50	3.50
	2.00	3.50	4.00	2.75	4.50	5.50	3.25
	3.25	2.50	3.50	2.50	3.25	4.50	2.75
	4.50	1.50	2.75	1.50	2.50	3.50	2.50
1.00	0.00	-	-	4.00	-	-	5.50
	0.42	6.25	6.25	4.00	9.00	9.00	5.50
	1.00	5.25	6.00	4.00	8.00	8.50	5.50
	2.00	4.25	5.25	3.50	7.00	7.50	5.25
	3.25	3.50	4.50	3.25	5.50	6.75	4.75
	4.50	2.75	4.00	2.75	4.50	5.50	4.50

TABLE XVIII

VACUUM RING DEFLECTION DATA
(TEST #6)

Conditions

1 in. Vacuum Ring	Clear Polyester Web
Static Crucifix	Surface Painted White
4 in. Wide	Line of Sight 0.0 deg.

		Tension X-Direction (lb/in)					
	Tension	(Light Source 35 deg.)			(Light Source 45 deg.)		
Vacuum (psi)	Y-Dir. (lb/in)	Same As Y	.42	4.5	Same As Y	.42	4.5
0.50	0.00	-	-	.0196	-	-	.0175
	0.42	.0321	.0321	.0196	.0375	.0375	.0175
	1.00	.0286	.0303	.0196	.0288	.0325	.0175
	2.00	.0250	.0286	.0196	.0225	.0275	.0163
	3.25	.0179	.0250	.0178	.0163	.0225	.0138
	4.50	.0107	.0196	.0107	.0125	.0175	.0125
1.00	0.00	-	-	.0286	-	-	.0275
	0.42	.0446	.0446	.0286	.0450	.0450	.0275
	1.00	.0375	.0428	.0286	.0400	.0425	.0275
	2.00	.0303	.0375	.0250	.0350	.0375	.0262
	3.25	.0232	.0321	.0232	.0262	.0338	.0238
	4.50	.0196	.0286	.0196	.0225	.0275	.0225

TABLE XIX

VACUUM RING FRINGE COUNT DATA
(TEST #7)

Conditions

Static Crucifix	Clear Polyester Web
4 in. Wide	Surface Painted White
X-Direction Tension .42 lb/in	Line of Sight 0.0 deg.
	Light Source 35 deg.

Tension Y-Dir. (lb/in)	1.5 in. Diameter Ring Vacuum (psi)			2 in. Diameter Ring Vacuum (psi)		
	.25	.50	1.00	.25	.50	.75
0.42	7.00	9.00	12.50	10.75	13.50	B
1.00	6.00	8.00	11.50	9.75	12.50	15.00
2.00	5.00	7.00	10.00	8.75	10.75	14.00
3.25	4.00	6.00	9.00	7.25	10.50	13.00
4.50	3.50	5.00	8.00	6.75	8.50	12.00

B - Web Buckled

TABLE XX

VACUUM RING DEFLECTION DATA
(TEST #7)

<u>Conditions</u>

Static Crucifix
4 in. Wide
X-Direction Tension .42 lb/in

Clear Polyester Web
Surface Painted White
Line of Sight 0.0 deg.
Light Source 35 deg.

Tension Y-Dir. (lb/in)	1.5 in. Diameter Ring Vacuum (psi)			2 in. Diameter Ring Vacuum (psi)		
	.25	.50	1.00	.25	.50	.75
0.42	.0500	.0643	.0892	.0768	.0964	B
1.00	.0428	.0571	.0821	.0696	.0892	.1071
2.00	.0357	.0500	.0714	.0625	.0768	.1000
3.25	.0286	.0428	.0643	.0518	.0750	.0928
4.50	.0250	.0357	.0571	.0482	.0607	.0857

B - Web Buckled

TABLE XXI

VACUUM RING FRINGE COUNT DATA
(TEST #8)

Conditions
1 in. Vacuum Ring
Static Crucifix
4 in. Wide
Y-Direction Tension 0.0 lb/in

Polypropylene Web
Line of Sight 22.5 deg.
Light Source 45 deg.

Tension X-Dir. (lb/in)	.25 psi Vacuum Web Width (in.) 6	4	.50 psi Vacuum Web Width (in.) 6	4	4*	4**
0.28	9.25	-	15.0+	-	-	-
0.42	-	8.75	-	15.0+	5.75	11.0+
0.67	8.25	-	13.0+	-	-	-
1.00	7.50	7.25	12.0+	14.0+	5.25	11.0+
1.33	6.75	-	11.0+	-	-	-
1.50	-	6.25	-	12.0+	4.50	9.00
1.67	6.00	-	10.0+	-	-	-
2.00	5.25	5.25	9.25	10.0	4.25	7.00
2.33	4.75	-	8.50	-	-	-
2.50	-	4.25	-	8.00	3.75	6.25
2.67	4.25	-	8.00	-	-	-
3.00	4.25	3.50	7.25	6.75	3.25	5.25
3.25	-	3.25	-	6.25	3.25	4.75
3.33	3.75	-	6.50	-	-	-
3.50	-	3.25	-	5.75	2.75	4.25
3.67	3.50	-	6.00	-	-	-
4.00	3.25	2.75	5.50	5.25	2.50	3.75
4.33	3.00	-	5.00	-	-	-
4.50	-	2.50	-	4.50	2.25	3.25
5.00	-	2.50	-	4.00	2.00	3.00

* - Light @ 35 deg., Line of Sight 0.0 deg.
** - Light @ 45 deg., Line of Sight 0.0 deg.
\+ - Fringes difficult to read accurately.

TABLE XXII

VACUUM RING DEFLECTION DATA
(TEST #8)

Conditions

1 in. Vacuum Ring
Static Crucifix
4 in. Wide
Y-Direction Tension 0.0 lb/in

Polypropylene Web
Line of Sight 22.5 deg.
Light Source 45 deg.

Tension X-Dir. (lb/in)	.25 psi Vacuum Web Width (in.) 6	4	.50 psi Vacuum Web Width (in.) 6	4	4*	4**
0.28	.0327	-	.0529+	-	-	-
0.42	-	.0309	-	.0529+	.0410	.0550+
0.67	.0291	-	.0458+	-	-	-
1.00	.0265	.0256	.0424+	.0494+	.0375	.0550+
1.33	.0239	-	.0388+	-	-	-
1.50	-	.0221	-	.0424+	.0320	.0450
1.67	.0212	-	.0353+	-	-	-
2.00	.0186	.0186	.0326	.0353	.0303	.0350
2.33	.0168	-	.0300	-	-	-
2.50	-	.0150	-	.0282	.0268	.0312
2.67	.0150	-	.0282	-	-	-
3.00	.0141	.0124	.0256	.0238	.0232	.0262
3.25	-	.0115	-	.0221	.0232	.0237
3.33	.0132	-	.0229	-	-	-
3.50	-	.0115	-	.0203	.0196	.0212
3.67	.0123	-	.0212	-	-	-
4.00	.0115	.0097	.0194	.0185	.0179	.0188
4.33	.0106	-	.0176	-	-	-
4.50	-	.0088	-	.0159	.0161	.0163
5.00	-	.0088	-	.0141	.0143	.0150

* - Light @ 35 deg., Line of Sight 0.0 deg.
** - Light @ 45 deg., Line of Sight 0.0 deg.
\+ - Fringes difficult to read accurately.

APPENDIX D

DERIVATION OF RIVELLO'S DEFLECTION EQUATION

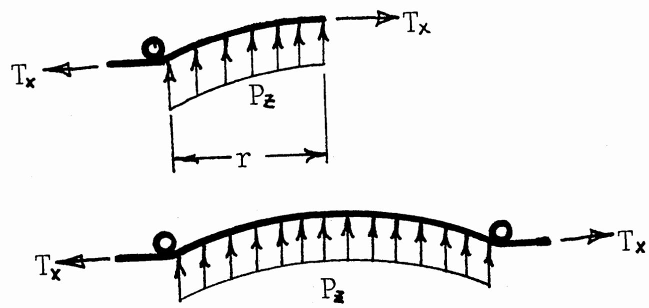

Figure 31. Rivello's Deflection Equation

<u>Calculations</u>

Governing Equation

$w'' = -P_z/T_x$

Boundary Conditions

$w'(r) = 0$

$w(0) = 0$

$w'' + P_z/T_x = 0$

Integrating

$w' + (P_z/T_x)x + C_1 = 0$

$(P_z/T_x)r + C_1 = 0$ @ $x = r$

$C_1 = -(P_z/T_x)r$

$w' + (P_z/T_x)x - (P_z/T_x)r = 0$

Intergrating

$w + (P_z/2T_x)x^2 - (P_z/T_x)rx + C_2 = 0$

$C_2 = 0$ @ $x = 0$

$w + (P_z/2T_x)x^2 - (P_z/T_x)rx = 0$

$w + (P_z/2T_x)r^2 - (P_z/T_x)r^2 = 0$ @ $x = r$

$w = P_z r^2/2T_x$ ***

VITA

Michael Allen Magill

Candidate for the Degree of

Master of Science

Thesis: CONTACTING WEB BIAXIAL STRESS TRANSDUCER

Major Field: Mechanical Engineering

Biographical:

Personal Data: Born in Fort Leonardwood, Missouri, May 29, 1958, the son of Vernon R. and Connie J. Magill. Married to Lisa L. Maeder on August 23, 1981.

Education: Graduated from Putnam City West High School, Bethany, Oklahoma, in May 1976; received Bachelor of Science Degree in Mechanical Engineering from Oklahoma State University in December, 1980; completed requirements for the Master of Science Degree at Oklahoma State University in July, 1988.

Professional Experience: Machinist, Induction Engineering/American Wind Turbine, Stillwater, Oklahoma, August, 1977, to Febuary, 1980; Summer Engineer, J.M. Huber Corporation, Borger, Texas, May, 1979, to August, 1979; Summer Engineer, Dow Chemical Company, Freeport, Texas, May, 1980, to August, 1980; Production Systems Engineer, Amoco Production Company, Rocky Mountain Region, January, 1981, to July, 1984; Instructor, Division of Engineering Technology, Oklahoma State University, August, 1984 to present.

Professional Organizations: Registered Professional Engineer for the State of Oklahoma, American Society of Engineering Educators, Society of Manufacturing Engineers.